BIBLIOGRAPHIC INFORMATION

PB95-124350

Report Nos:

Title: U.S.-TCCMAR 5-Story Full-Scale Masonry Research Building Test. Preliminary Report.

Date: Oct 92

Authors: F. Seible, G. A. Hegemier, M. J. N. Priestley, G. R. Kingsley, A. G. Kurkchubasche, and A. Igarashi.

Performing Organization: United States-Japan Coordinated Program for Masonry Building Research.**California Univ., San Diego, La Jolla. Dept. of Applied Mechanics and Engineering Sciences.

Sponsoring Organization: *National Science Foundation, Arlington, VA.

Contract Nos: NSF-ECE85-52672

Supplemental Notes: Also pub. as United States-Japan Coordinated Program for Masonry Building Research rept. no. REPT-9.2-4 and TR-92/01. See also PB93-214724.

NTIS Field/Group Codes: 89D (Structural Analyses), 89G (Construction Materials, Components, & Equipment)

Price: PC A04/MF A01

Availability: Available from the National Technical Information Service, Springfield, VA. 22161

Number of Pages: 68p

Keywords: *Earthquake resistant structures, *Masonry, *Earthquake damage, *Structural failure, Structural vibration, Earthquake engineering, Construction materials, Cracks, Displacement, Ductility, Buildings, Concrete slabs, Structural design criteria, Dynamic response, Walls, Damage assessment, Reinforcement(Structures), United States, International cooperation, Japan, *Masonry buildings.

Abstract: The first U.S. 5-story full scale building test under simulated seismic loads was conducted at the University of California, San Diego between July 28, 1992 and September 29, 1992. The full scale 5-story research building was a reinforced concrete masonry structure comprised of coupled flanged walls and precast, prestressed hollow-core plank floors with reinforced topping. This seismic simulation test was conducted as part of the U.S. Coordinated Program for Masonry Research, under the direction of the Technical Coordinating Committee for Masonry Research (TCCMAR), a program which involved numerous research teams, engineering consultants and industry observers. The charge to the TCCMAR group by the National Science Foundation was to develop and verify new design guidelines for masonry buildings in seismic zones. The research goal was accomplished through parallel analytical and experimental research programs conducted around the U.S. at the material, component, and structural subassemblage levels, culminating in the final validation and verification of TCCMAR analysis and design models by means of this 5-story full scale masonry building test.

米日

U.S. - JAPAN COORDINATED PROGRAM
FOR
MASONRY BUILDING RESEARCH

REPORT NO. 9.2-4

THE U.S.-TCCMAR 5-STORY FULL SCALE MASONRY RESEARCH BUILDING TEST - PRELIMINARY REPORT

by

FRIEDER SEIBLE
GILBERT A. HEGEMIER
M.J. NIGEL PRIESTLEY
GREG R. KINGSLEY
ALBERT G. KURKCHUBASCHE
AKIRA IGARASHI

OCTOBER 1992

supported by:

NATIONAL SCIENCE FOUNDATION

GRANT NO. ECE 86-03672

DEPARTMENT OF APPLIED MECHANICS & ENGINEERING SCIENCES
UNIVERSITY OF CALIFORNIA, SAN DIEGO

This report presents the results of a research project which was part of the U.S. Coordinated Program for Masonry Building Research. The program constitutes the United States part of the United States - Japan Coordinated Masonry Research Program conducted under the auspices of the Panel on Wind and Seismic Effects of the U.S.-Japan Natural Resources Development Program (UJNR).

This material is based on work supported by the National Science Foundation under the direction of Program Director, Dr. S.C. Liu.

Any opinions, findings, and conclusions or recommendations expressed in this publication are those of the authors and do not necessarily reflect the views of the National Science Foundation and/or the United States Government.

University of California, San Diego
Structural Systems Research Project

Report No. TR-92/01

THE U.S. - TCCMAR 5-STORY FULL-SCALE MASONRY RESEARCH BUILDING TEST

by

Frieder Seible[1]
Gilbert A. Hegemier[2]
M.J. Nigel Priestley[1]
Gregory Kingsley[3]
Albert Kürkchübasche[3]
Akira Igarashi[3]

[1]Professor of Structural Engineering
[2]Professor of Applied Mechanics
[3]Graduate Research Assistant

Department of Applied Mechanics and Engineering Sciences
University of California, San Diego
La Jolla, California 92093-0411

October 1992

THE U.S.-TCCMAR 5-STORY FULL SCALE MASONRY RESEARCH BUILDING TEST, PRELIMINARY RESULTS

Table of Contents

THE U.S.-TCCMAR 5-STORY FULL SCALE MASONRY RESEARCH BUILDING TEST, PRELIMINARY RESULTS

1 INTRODUCTION

The first U.S. 5-story full scale building test under simulated seismic loads was conducted at the University of California, San Diego between July 28, 1992 and September 29, 1992. The full scale 5-story research building was a reinforced concrete masonry structure comprised of coupled flanged walls and precast, prestressed hollow-core plank floors with reinforced topping. This seismic simulation test was conducted as part of the U.S. Coordinated Program for Masonry Research, under the direction of the Technical Coordinating Committee for Masonry Research (TCCMAR), a program which involved numerous research teams, engineering consultants and industry observers. The charge to the TCCMAR group by the National Science Foundation was to develop and verify new design guidelines for masonry buildings in seismic zones. This research goal was accomplished through parallel analytical and experimental research programs conducted around the U.S. at the material, component, and structural subassemblage levels, culminating in the final validation and verification of TCCMAR analysis and design models by means of this 5-story full scale masonry building test.

The principal test objectives for the full scale building test were:

(1) To provide a test bed for the TCCMAR design philosophy and design models,
(2) to provide benchmark data for TCCMAR analysis procedures, and
(3) to advance the state-of-the-art in full scale laboratory testing of stiff multi-degree-of-freedom structures under simulated seismic loads.

Specific performance criteria established for the building were:

(1) To develop dependable displacement ductility up to four times yield displacement without excessive strength or stiffness degradation,
(2) to dissipate seismic energy by ductile inelastic modes of response, and
(3) to inhibit brittle modes of inelastic displacement, such as shear failure or bond failure by a capacity design approach. This requires, for example, that the shear strength of all parts of the walls must exceed the maximum shear force corresponding to development of flexural overstrength, including the effects of variable shear/moment ratios at critical sections resulting from higher mode effects.

To meet the general TCCMAR design philosophy of ductile behavior, a test structure was selected with a structural configuration which inherently allows ductile behavior through the formation of plastic hinges at the base of shear walls and in the beam or coupling elements.

The simulated seismic load tests were conducted with ten servo-controlled hydraulic actuators (two per floor level) utilizing the Generated Sequential Displacement (GSD) procedure, an on-line testing technique based on pseudo-dynamic testing principles. While it is beyond the scope of this preliminary test report to describe the experimental control, it is important to point out that the GSD method developed at UCSD allowed for the pseudo dynamic testing of the stiff, undamaged reinforced masonry research building from the very beginning, and that all structural damage incurred by the test specimen was inflicted by simulated seismic load input and not by predetermined lateral load distribution patterns, which makes this the first world-wide full scale 5-story test of a stiff shear wall building under seismic load input.

In the following, a brief overview of the geometry and the design of the test structure will be presented, followed by a descriptive summary of the experimental test sequence and the observed structural behavior with increasing seismic excitation levels. Key test results will be presented in the form of total base shear versus top building displacements to judge the overall performance of the structure, and typical response data for a pseudo dynamic GSD time window will be presented to illustrate the employed testing procedure. Finally, the performance criteria established prior to the test by TCCMAR will be compared with the experimental results to establish the degree to which the research building met or exceeded the performance goals.

This preliminary test report will be followed by a comprehensive research report which will discuss in detail the GSD test procedure, the analytical predictions, diagnostic analyses, and final post-test models, as well as a complete documentation of all the material quality control tests, and the experimental test data which are currently being reduced from over 500 instruments monitored during a total of 75 independent tests. Finally, the seismic performance of the test specimen will be evaluated and documented by TCCMAR with respect to the developed analytical models and design criteria for masonry buildings in seismic zones.

2 GEOMETRY AND DESIGN OF THE TEST SPECIMEN

A complete description of the test specimen, including construction documents, the justification for the chosen geometry, and a detailed discussion of the design can be found in reference [6]. A photo documentation of the construction and testing of the 5-story research building is given in Appendix A. In the following, the building geometry will be described briefly, and salient features of the design will be reiterated to demonstrate the underlying design philosophy, particularly as it relates directly to the building response discussed in Chapters 5 and 6.

The primary design basis for the 5-story reinforced masonry research building was the NEHRP Recommended Provisions for the Development of Seismic Regulations for New Buildings [1,2], including a proposed Appendix to Chapter 12 for Masonry [3,4,5]. At the time of the design, these standards represented the most complete implementation of TCCMAR research results in a coherent standard, and they provided a platform for the development of the TMS Draft Masonry Limit Design Standard. Where conditions arose that were not addressed specifically in these documents, the fundamental principles of capacity design were applied [7], or results from TCCMAR or related research were utilized directly.

2.1 Building Geometry

The 5-story masonry research building, illustrated in Figure 1, represents an isolated segment of a typical medium rise reinforced masonry (RM) apartment or hotel structure and is intended to capture the essential characteristics of the lateral load resisting system in such a structure. It consists of two cantilever shear walls of unequal length, each with a 16'-8" flange, coupled by topped precast pre-tensioned hollow-core concrete plank floor slabs (Figure 2). The longer wall is L-shaped in plan and has a length in the plane of loading of 13'-4". The shorter of the two walls is T-shaped in plan, with the flange located at the center of the 7'-4" long web. The long flanged wall has a highly asymmetrical response in the two loading directions: when the flange is in compression, the large compression area allows the development of very high ductility; when the flange is in tension, the large area of tension reinforcement in the flange results in the development of high ultimate moments, but low curvature ductility. In the absence of coupling effects, the short T-shaped wall would exhibit symmetrical behavior in each loading direction.

Coupling between the two shear walls is provided by the precast, prestressed hollow-core concrete floor slabs topped with a 2-inch thick cast-in-place reinforced concrete topping. Typically, structural masonry shear walls would also be coupled by structural lintels over the door openings. In the research building, the door openings were spanned by a non-structural lintel separated from the adjacent walls by a fire rated expansion joint to allow the slab to rotate relative to the walls without engaging the lintel, thus coupling was provided only by bending in the 8-inch concrete floor slab system.

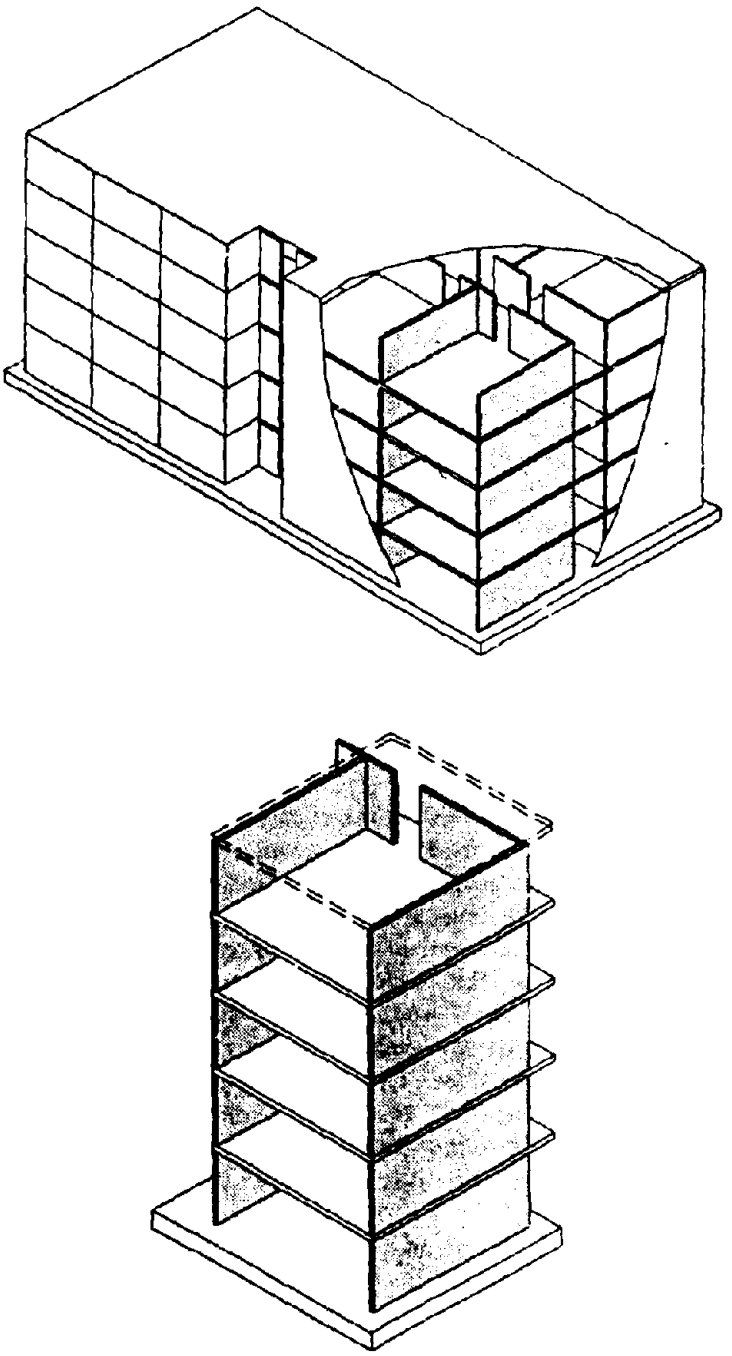

Figure 1 5-Story Reinforced Masonry Research Building (a) Prototype (b) Test Structure

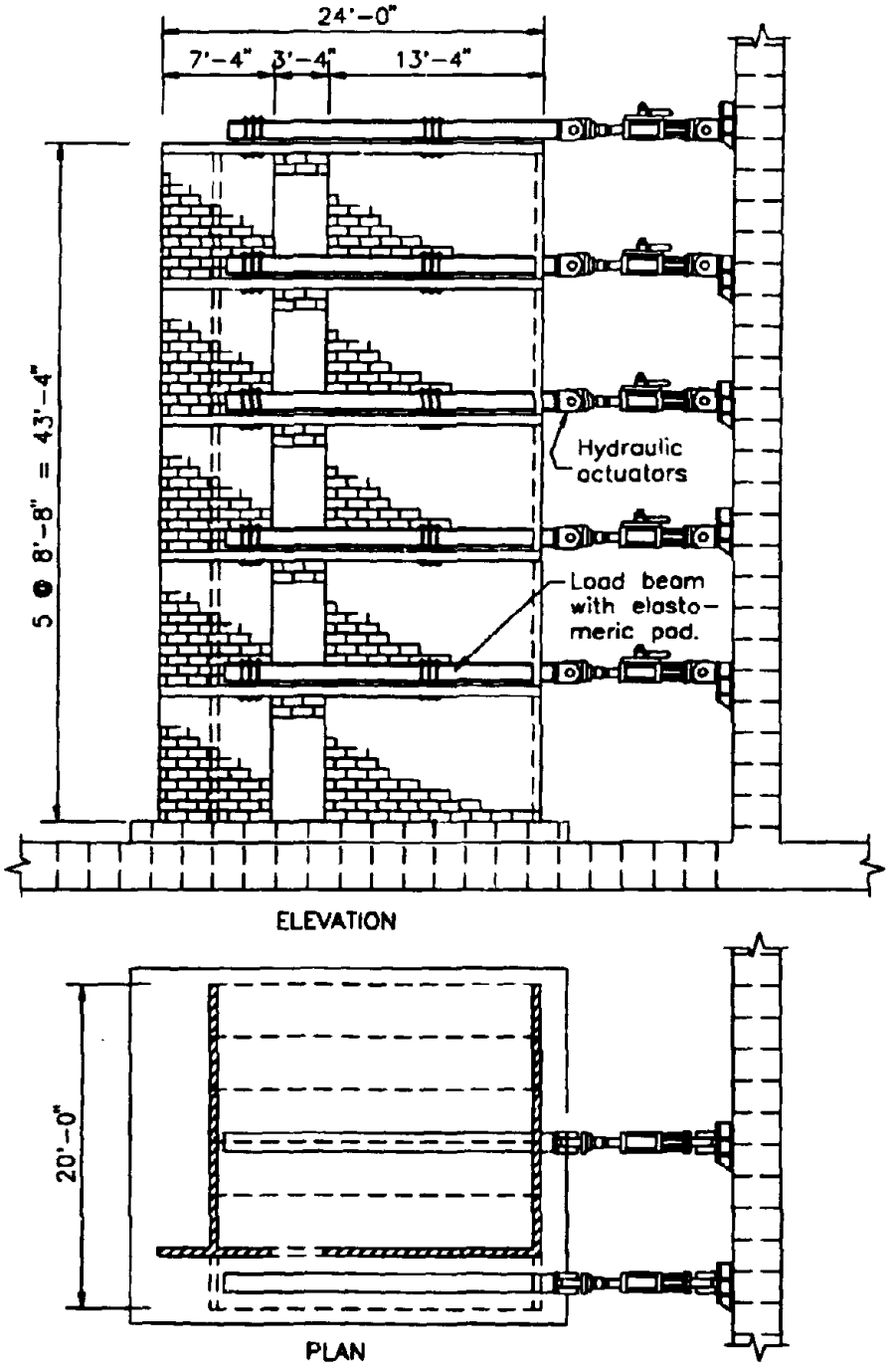

Figure 2 5-Story Reinforced Masonry Research Building, Plan and Elevation

2.2 Lateral Force Resisting System

The seismic lateral force resisting system of the coupled shear wall test structure may be described in terms of the total overturning moment, which is comprised of the individual contributions of the shear walls and the coupling system:

$$M_{ot} = M_1 + M_2 + A * l \tag{1}$$

The terms M_1 and M_2 represent the portions of the overturning moment carried by the short T-section and long L-section walls respectively. The term $A*l$ represents the contribution of the coupling system, where A is the sum of the coupling shears in the 5 floors, and l is the moment arm between the lines of action of the wall axial forces, A. In the design of the coupled wall system, it is important to consider not only the moment capacity of each wall under the imposed dead loads and lateral forces, but also the effect of wall axial loads introduced by the coupling system, and the resulting amplification of the total overturning moment.

As the coupling shears increase, the wall axial load increases, and thus the required flexural reinforcement decreases. This issue is not explicitly addressed in building codes. In order to avoid under-reinforcement of the walls, the flexural design of the walls was based on a maximum coupling shear associated with the first yield in the slabs [6].

2.3 Reinforcement Details

Reinforcing details for the shear walls and flange walls are given in Figures 3 and 4. Vertical reinforcing in both long and short shear walls consisted of #5 bars at 16" on center in the first three stories, and #4 bars at 16" on center in the fourth and fifth stories. Bar sizes were kept as small as possible, and were uniformly distributed throughout the walls to facilitate construction and grouting of the walls, and to promote the development of well distributed cracks in the plastic hinge zones.

Design of the vertical reinforcement for the flanges was initially based on an analysis for seismic loads in the plane of the flanges, and resulted in a requirement for only code minimum reinforcement in these walls. However, design for forces in the plane of the webs indicated the need for additional reinforcement in the flanges to ensure that, when the flange was in tension, the ultimate flexural strength would exceed the cracking strength, thus encouraging the formation of well distributed cracks in the plastic hinge region. This resulted in a requirement for #4 bars at 16" on center for the first three stories, and #4 bars at 32" on center for the top two stories.

In order to avoid the development of nonductile failure mechanisms associated with rebar bond failure, no lap splices were permitted in the first story of the structure. The use of single-open-end bond-beam block units facilitated the placement of blocks around the story-height reinforcement at the first level. Above the first story, reinforcement lap splices, 24", (or approximately 40 bar diameters), in length, were located just above each floor level.

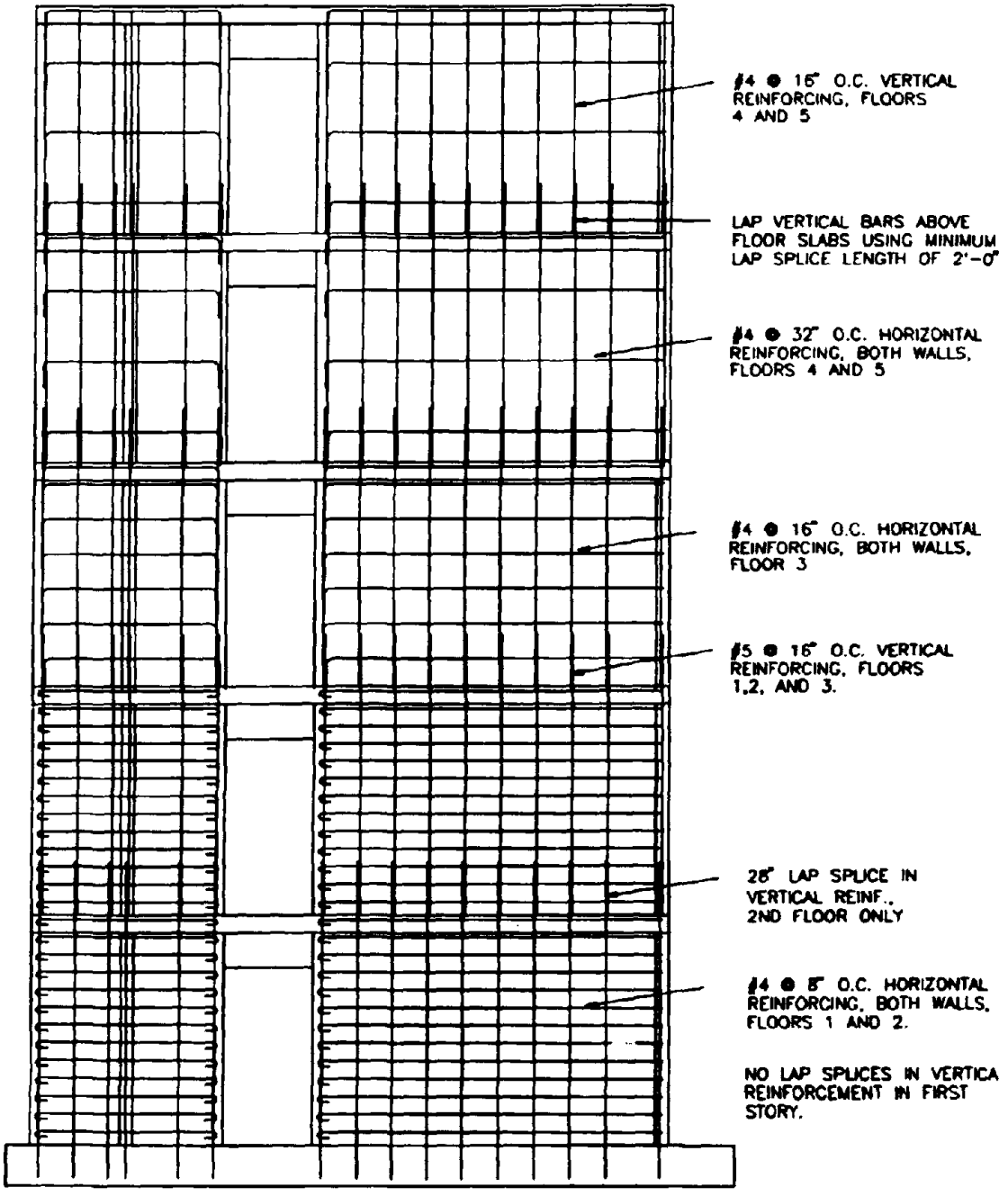

Figure 3 Reinforcing in Long and Short Shear Walls

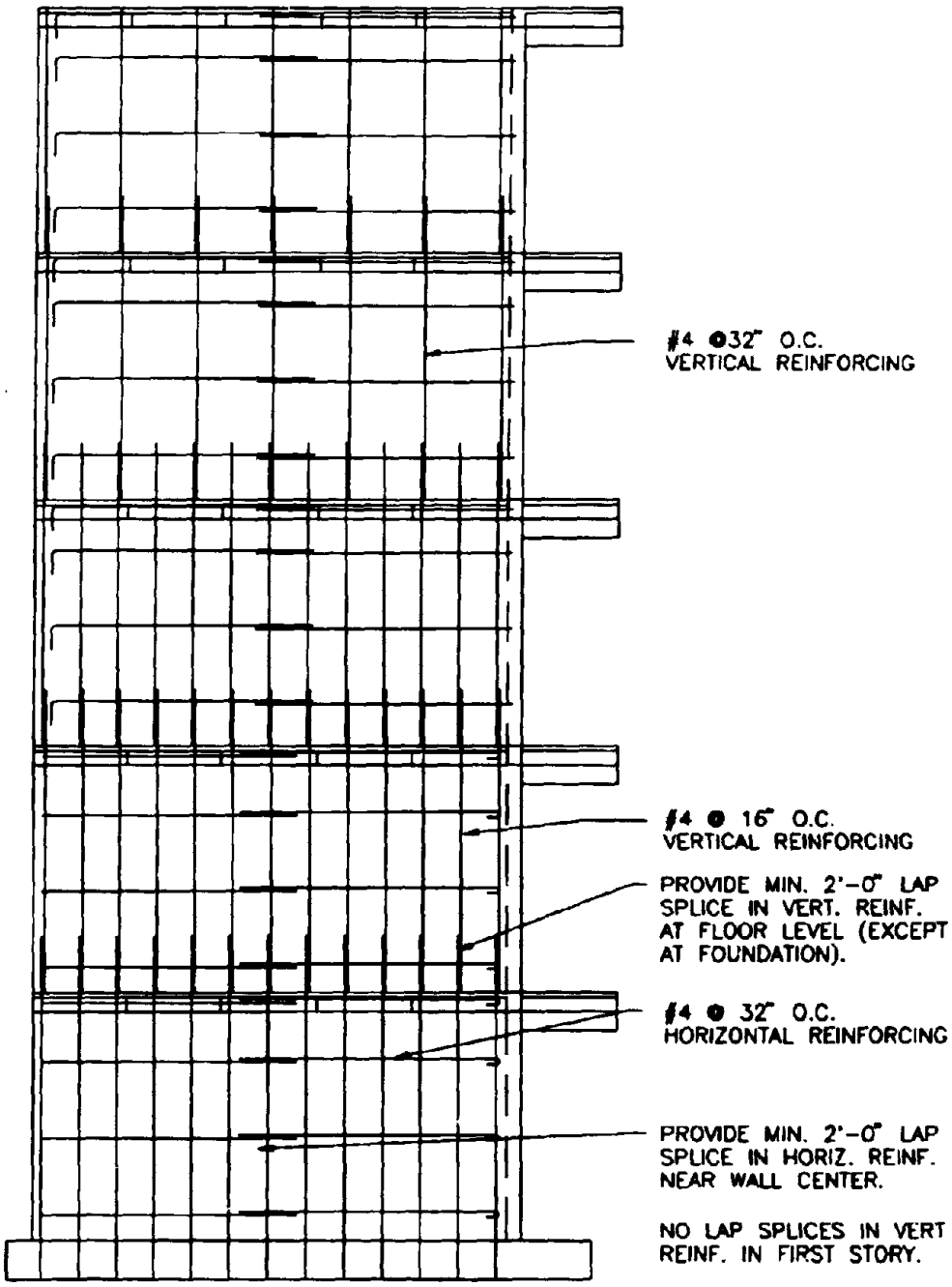

Figure 4 Reinforcing in Flange Walls

Horizontal reinforcement was designed for the condition when the full over-strength moment of the long wall with the flange in tension was achieved. The required shear strength was amplified by appropriate material overstrength factors and a dynamic amplification factor equal to 1.4 to account for the magnification of the base shear due to higher mode effects. This resulted in a requirement for #4 bars at 8" on center for the first two stories, #4 bars at 16" on center for the third story, and #4 bars at 32" on center for floors 4 and 5. Horizontal reinforcement in the flanges is at code minimum level, and the spacing is the minimum allowed in the NEHRP provisions.

The precast, hollow core planks were pretensioned on the bottom face with 4 straight 3/8" diameter, 270 ksi prestressing tendons. The two inch cast in place topping was reinforced with #3 bars at 16" on center parallel to the shear walls, and #4 bars at 18" on center perpendicular to the shear walls (see Figure 5).

In the coupling region, (between the walls and between the planks on either side of the walls), 4 #3 bars with tightly spaced stirrups (see Figure A-3) were provided to (a) transfer the shear across the coupling region, and (b) confine the concrete in the plastic hinge zones adjacent to the walls. The lintel below the coupling region contained code-minimum reinforcement, and was separated from the walls on either side by 1/2 inch movement joints to allow free rotation of the slab without engaging the lintel.

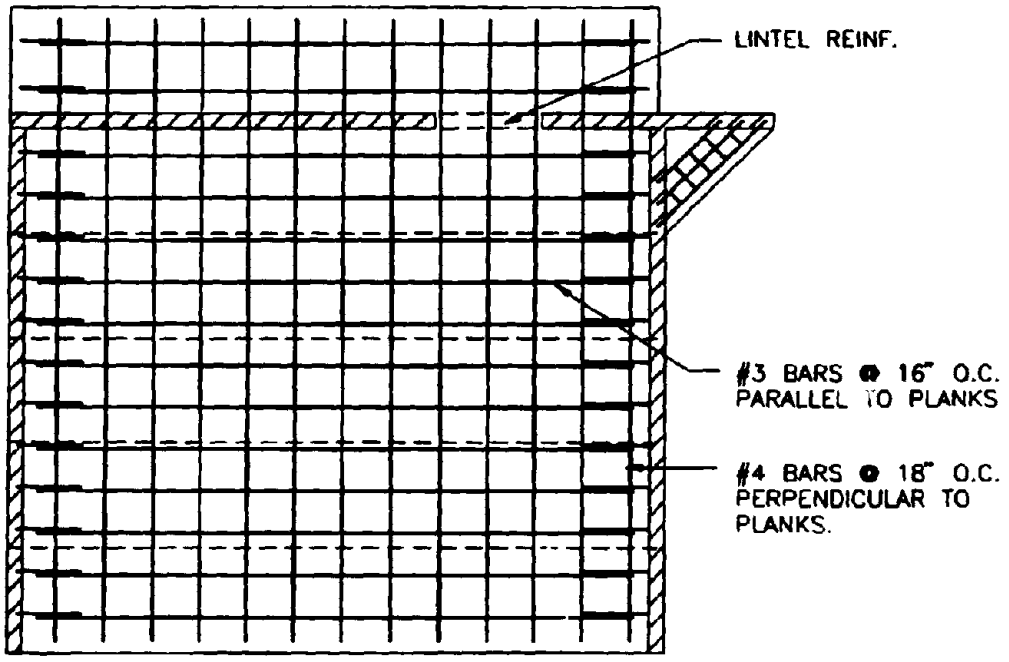

Figure 5 Reinforcement of the Slab Topping

2.4 Estimated Structural Stiffness and Strength

In order to develop an accurate estimate of the structural stiffness and strength, several factors must be considered:

(1)Effective slab width,
(2)effective flange wall width,
(3)cracked and uncracked properties of walls and slabs, and
(4)height of the effective plastic hinge zone in the shear walls.

The choice of effective widths for the slabs and flanged walls was based directly on the results of TCCMAR research tasks [8,9]. Slabs were assumed to have an effective width equal to one precast plank width on either side of the shear walls, or a total width of 86 inches. The flange walls were assumed to contribute half of their total width (100 inches) at first cracking, and their entire width (200 inches) following yielding of the reinforcing. Cracked stiffness properties for the walls were estimated using the recommendations of Priestley and Hart [10].

Calculation of the wall stiffness following yielding requires the estimation of the height of the plastic hinge zone above the base. Plastic hinge lengths for the short and long walls were taken as 33 inches and 47 inches respectively, using a simple relationship which depends on the wall length l_w and the effective height of the structure h_e :

$$l_p = 0.2l_w + 0.04h_e \qquad (2)$$

2.5 Predicted Behavior Characteristics

For the purpose of estimating the period of vibration, design gravity loads were based on the tributary floor areas in the *prototype* structure (Figure 1a). This resulted in a total building weight of 410 kips. The distribution of building mass and the equivalent static lateral load distribution are shown in Figure 6. Based on these values, the effective height of an equivalent single degree-of-freedom structure is 31'-2". The *test* structure (Figure 1b) has less mass than the prototype structure, since no additional mass was provided to represent the dead loads or the additional floor area in the prototype structure. The total weight of the test structure was 284 kips. While the larger dead loads associated with the prototype structure were used in calculation of the building period and the equivalent static lateral loads, the smaller loads were considered in the design of the walls.

The period of vibration of the structure was estimated using a linear elastic equivalent frame analysis. Predicted periods for 5 modes of vibration, based on the total seismic mass discussed above, will be given in Section 5 and compared with experimental data for two structure limit states. For purposes of design, a first mode period of T=0.3 seconds was selected to represent a reasonable estimate of the cracked section period of the structure.

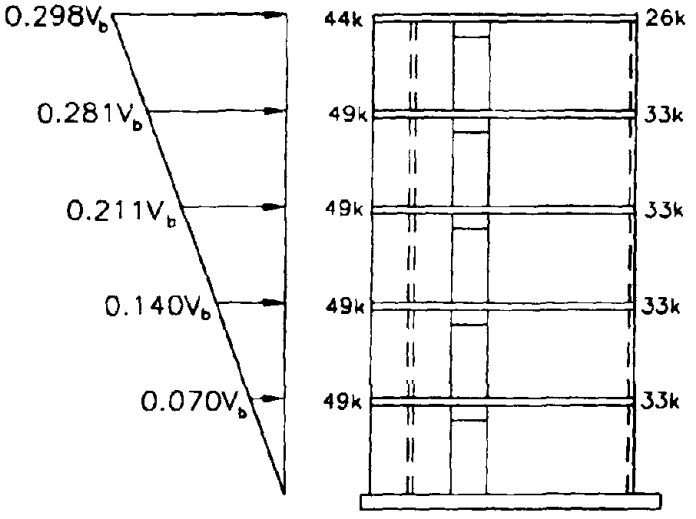

Figure 6 Equivalent Lateral Load Distribution and Tributary Weight at Floor Levels

The design base shear (V_b) was calculated based on sections 4.1 and 4.2 of the NEHRP seismic design provisions, giving:

$$V_b = 0.222 * 410 \ kips = 91 \ kips \qquad (3)$$

It should be noted that a Response Modification Factor of 4.5 (recommended for RC walls) was used, rather than the NEHRP recommended value of 3.5 for RM walls.

A piecewise linear analysis using beam-type elements was performed to identify the development of plastic hinges in the slabs and walls, the collapse mechanism, and the expected ultimate capacity of the structure. Results of the final analysis are presented in Figure 7 in terms of base overturning moments. This figure illustrates the predicted response in terms of the contributions from each wall and the coupling forces.

In Figure 8, the predicted capacity is shown again in terms of base shear along with the design level capacity, and a nonlinear finite element prediction of the lateral load deformation response. The finite element model represents one of the advanced analytical models for reinforced masonry systems developed as part of the TCCMAR program.

The predicted ductility levels based on idealized bilinear response for both the design (subscript d) and actual performance (subscript p) levels are illustrated in Figure 8. The design ductility capacity (11.1 in the weak direction when the long wall flange is in compression, or 5.8 when the flange is in tension) reflects the fact that the force demand on the structure is less than the predicted capacity. The performance ductility capacity

(5.4 in the weak direction and 2.2 in the strong direction) is independent of the expected demand on the structure, and is therefore a property of the structure alone; however, it neglects the potential benefit of overstrength which effectively reduces the ductility demand.

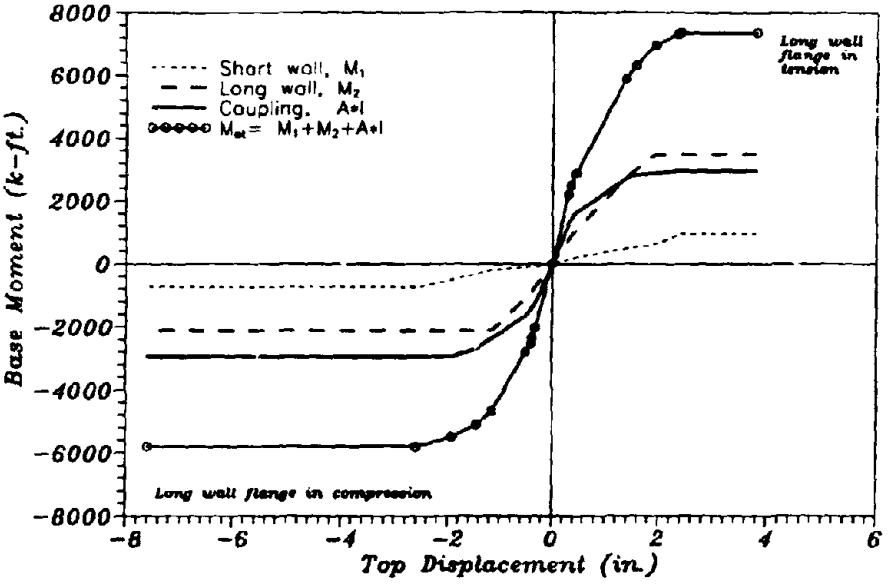

Figure 7 Predicted Response of Individual Walls and Complete Structure Including Coupling Effects

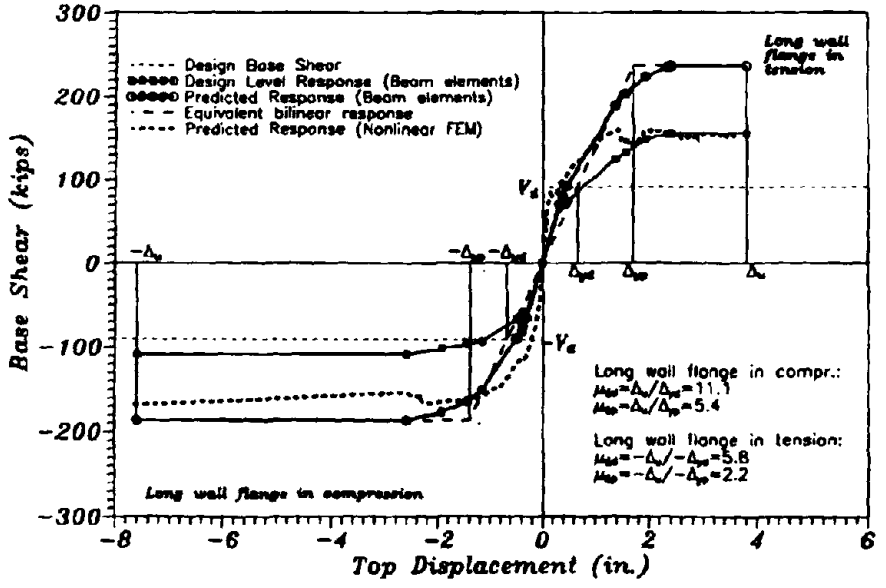

Figure 8 Predicted Response and Design Level Response Incorporating Strength Reduction Factors

3. CONSTRUCTION, INSTRUMENTATION, AND TEST PLAN

3.1 Construction of the Research Building

Complete construction drawings and specifications for the 5-story masonry research building have been presented in reference [6], and the construction process will be thoroughly documented in the follow up report. A brief outline of the construction sequence is presented here, with photo references in Appendix A. Construction of the specimen was performed by professional contractors and supervised by laboratory staff. Insofar as possible, construction procedures and details were consistent with standard practice for the industry.

1) The 18" deep RC foundation was cast in place (see Figure A-1a) and post-tensioned to the test floor using 55 1-1/4" diameter Grade 150 bars tensioned to 100 kips each. Vertical reinforcing bars for the first story masonry walls, extending 11'-0" above the top of the foundation, were anchored in the foundation. The top of the concrete footing was roughened under the locations of the masonry walls, and 1-1/2" deep by 3-1/2" wide shear keys were provided at 16" intervals.

2) The masonry walls were constructed using nominal 6"x8"x16" concrete masonry units. All units (excepting those at the ends of the walls) were single open-ended (A-shaped) bond beam blocks to facilitate both the initial construction and the horizontal flow of grout throughout the walls. The first course of masonry units had clean-out holes located at every vertical bar (see Figure A-1b). These were cleaned with compressed air and sealed prior to grouting. Shoring was provided for the construction of non-structural lintels over the doorways (Figure A-2). Faceshells of the flange/wall intersections were cut to allow horizontal flow of grout through the joint.

3) Walls were grouted in two lifts to a height 4" from the top of the wall using a coarse (3/8" maximum aggregate) grout with an expansive admixture to counteract shrinkage. Grout was consolidated using a mechanical vibrator over the full story height.

4) Temporary shoring was constructed to support the single floor plank on the East side of the shear walls opposite the flanges. Precast, pretensioned hollow-core concrete planks were placed, bearing on the faceshells of the flanged walls and on the temporary shoring on the side opposite the flanges (see Figure A-2). Joints between the planks and at the plank/wall interface were sealed on the bottom face and then grouted with a cement/sand grout.

5) Edge forms were constructed around the floor slabs. Topping reinforcement, and the reinforcement in the coupling region over the lintels was tied in place (see Figure A-3). RC beams were formed to support the plank opposite the flanges.

6) Cast-in-place concrete topping was placed with a depth of 2" maintained at the location of the door opening. The surface of the concrete was roughened at the locations of the masonry walls.

7) The above sequence, beginning at step 2 was repeated for each of the remaining stories. The completed test specimen is pictured in Figure A-4.

As shown in Figure 2, loads were transmitted to the structure at each floor slab by two actuators used in parallel, thus allowing the imposition of displacements on the floor slabs without inducing structural torsion. The loads were transmitted from the actuators to the floor slab through load distribution beams and two elastomeric bearing pads (see Figure A-5). By virtue of reducing the apparent stiffness of the floor slab, this arrangement provided approximately uniform load distribution between the loading areas. The pads also provided a mechanical amplification of the structural displacements to be imposed, an important element of the GSD testing procedure. Furthermore, they allowed for limited unconstrained structural rotations and expansions, protection of the structure from actuator instabilities during shake down tests, and a reduction in coupling stiffness between active DOFs.

3.2 Instrumentation and Data Processing

Instrumentation for the 5-story research building was selected to provide the experimental data required for analysis and design model verification. The instrumentation can be divided into the following classifications:

(a) Actuator displacements and loads.
(b) Displacement of the floor slabs.
(c) Wall panel deformation.
(d) Slip and separation between wall panels and slabs
(e) Lintel rotation.
(f) Curvature of wall panels.
(g) Slip between floor planks.
(h) Transverse wall displacements.
(i) Rebar strain.

The global systems instrumentation consisted of ten load cells and LVDTs associated with the ten servo-controlled actuators. An additional set of 20 LVDTs, which monitored the actual test structure deformations referenced to independent instrumentation columns at the 5-story levels, comprised the feedback control instrumentation for the on-line testing procedure.

Figure 9 shows the location of the primary displacement measurement devices (a-f above). In addition to the feedback control instrumentation, linear potentiometers or LVDTs monitored overall vertical and torsional deformation modes of the test structure. Each floor level had two wall panels, and the deformation of each wall panel was measured using five LVDTs as shown in Figures 9, A-6, and A-7. The method of deriving the five independent modes of wall panel deformation from these LVDT measurements is described in reference [11]. Curvature profiles at the base of the walls were measured using curvature gages fixed to the wall edges. Three LVDTs were provided on the lintels at each floor level to measure the rotation of the floor slabs relative to the walls, and the extension of the floor slab spanning the door. Instruments were also provided to measure

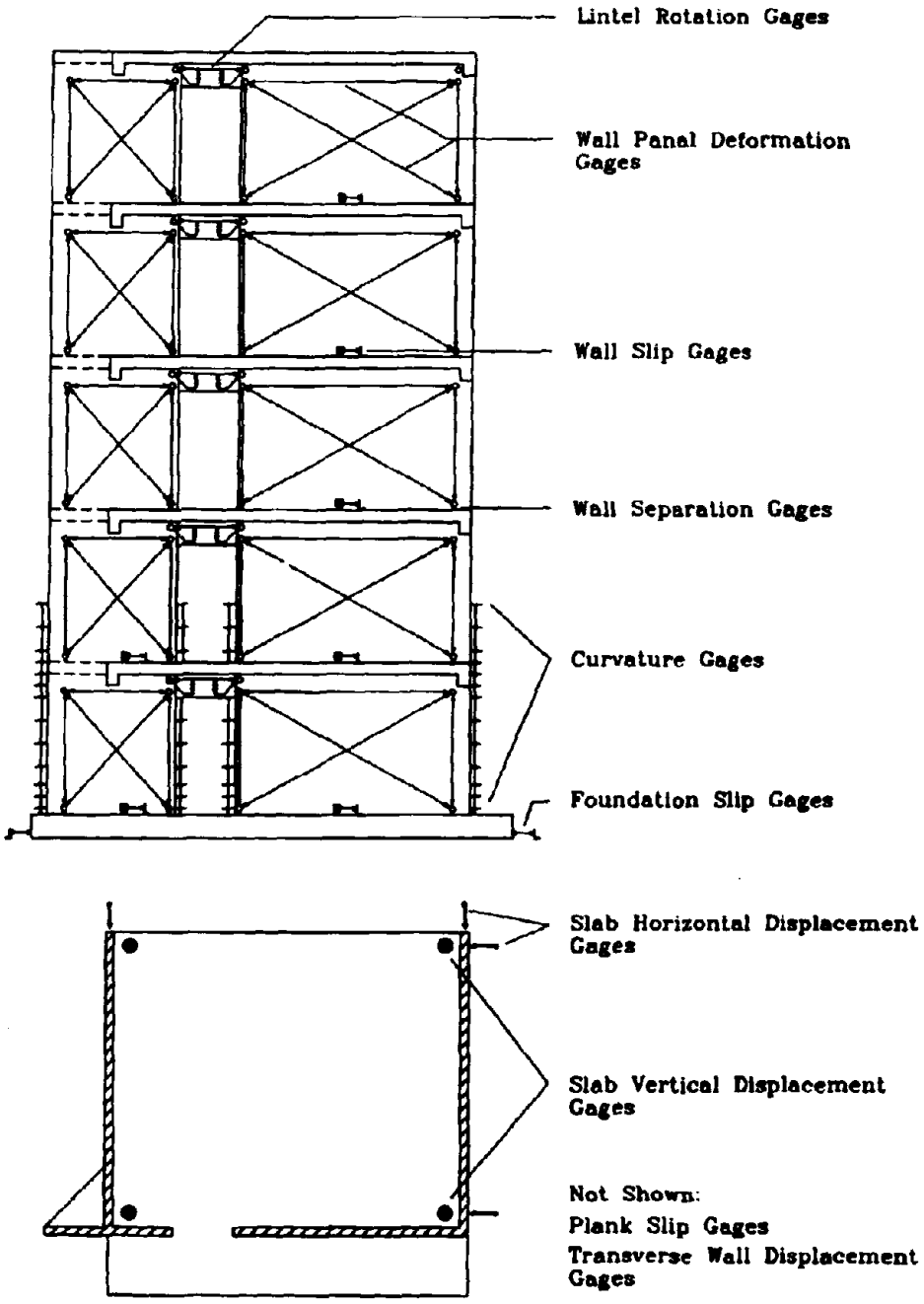

Figure 9 Overview of Building Component Instrumentation

the slip and separation of each wall panel relative to the floor slab below. Not shown in the figure are the instruments which monitored slip between the precast floor planks, and out-of-plane deformations of the shear walls.

Reinforcement in each component was instrumented with strain gages to determine yield onset, neutral axis locations, and approximate component stress states as shown in Figure 10.

During the tests, the current state of the specimen was continuously displayed in real time to monitor test progress. The real time data display system included graphic representations of (1) time vs. measured displacement for each floor, (2) base shear vs. top displacement, (3) base moment vs. top displacement, (4) overall deformed shape of the specimen and load distribution, (5) hysteretic behavior of wall panel components, and (6) curvature profiles. In addition, the real time displacement response was compared to the prediction obtained from elastic linear dynamic analysis based on measured pretest structural stiffness.

3.3 Test Plan

The experimental test plan for the 5-story RM research building was designed to subject the structure to progressively increasing damage states resulting from forces induced by simulated earthquake ground motions, while simultaneously tracking the stiffness degradation, energy absorption, and hysteretic characteristics of the structure. In order to achieve this objective, four types of tests were conducted:

Generated Sequential Displacement Test (GSD): An on-line testing technique, based on pseudo dynamic testing principles, that combines analytical dynamic analyses with experimental methods to allow testing of stiff, multi degree-of-freedom structural systems under simulated seismic loads. The procedure, developed at UCSD, is described in detail in references [6,11]. Selection of input ground motions is discussed briefly below.

Inverse Triangular Load Test (ITL): A quasi-static cyclic load test in which the structure was subjected to a predefined inverse triangular load distribution through one complete cycle up to, but not exceeding, the maximum displacement attained in the previous GSD test. No new damage was inflicted on the structure during ITL tests.

Conventional Stiffness Test: A stiffness measurement techniqe in which each of the 5 degrees of freedom are displaced while holding the others fixed to measure the structural stiffness matrix. Displacement levels are held below very low limits. This type of test was only conducted as part of the initial shakedown tests.

Modal Stiffness Test: An alternative stiffness measurement technique in which the 5 degrees of freedom are displaced together into each of 5 linearly independent mode shapes to allow the calculation of the structural stiffness matrix.

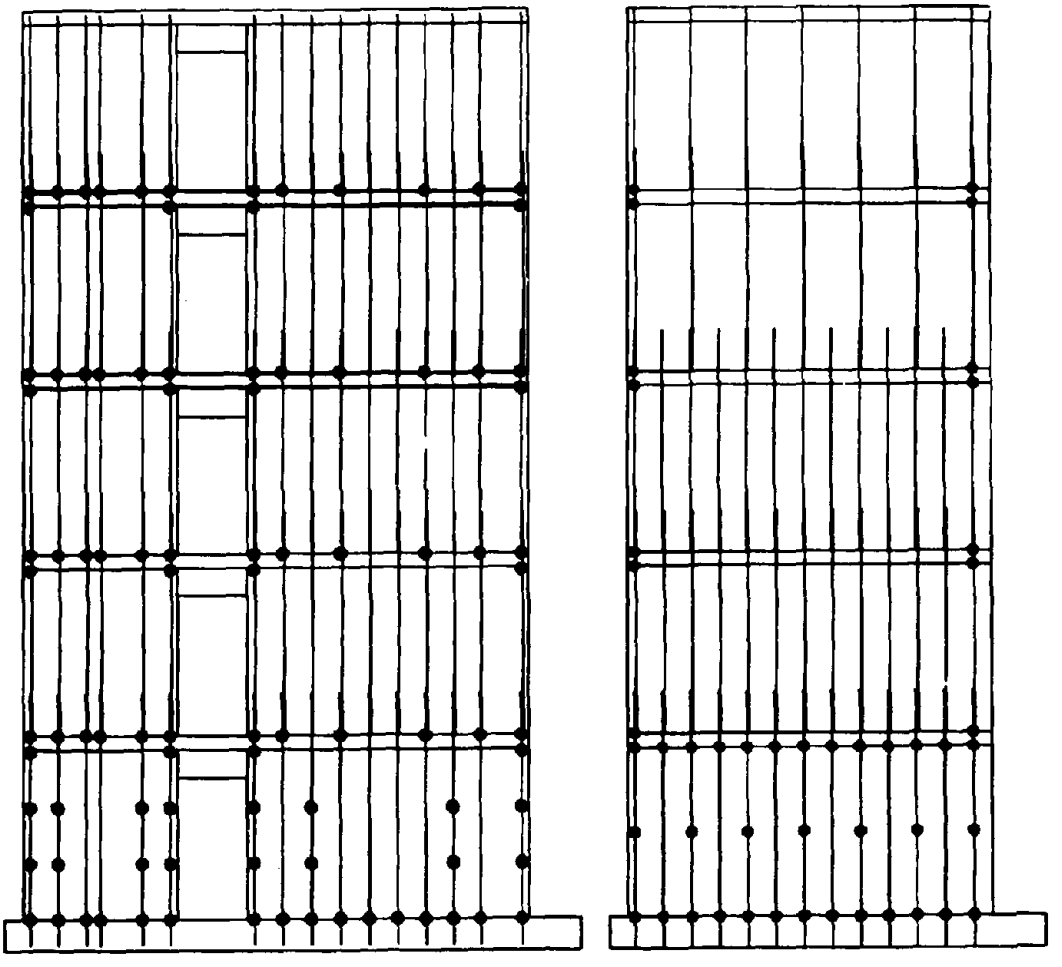

Location of Strain Gages in Shear Walls Location of Strain Gages in Flange Walls

Figure 10 Overview of Reinforcing Bar Strain Gage Location

Testing began with a series of initial hardware and software shakedown tests. These consisted primarily of Conventional and Modal Stiffness tests designed to measure the initial uncracked stiffness of the structure, and very low level GSD tests conducted to test the stability and convergence rate of the GSD testing algorithm, and to measure the seismic response of the undamaged structure. Following the shakedown tests, tests on the research building were carried out in a regular sequence. First, a GSD test was conducted using an earthquake acceleration record window chosen specifically to take the structure to the next desired limit state. The maximum displacement attained was generally limited to 150% of the previous maximum response. Each GSD test was then followed by a single-cycle ITL test to the previous GSD top displacement, without introducing any additional damage to the test structure, to allow measurement of the stiffness and hysteretic response of the structure under first mode load distributions. During the ITL tests, the structure was held stationary for 15-20 minutes at the maximum positive and negative displacements to allow for inspection of damage and marking of cracks. Following the ITL test, a Modal Stiffness test was conducted to precisely quantify the current stiffness of the 5-dof structural system.

Table 1 Proposed Earthquake Record Windows

Ground Motion	Window (5 sec.)	scale factor	Remarks
San Fernando 1971 Hollywood Storage P.E. Lot N90E	2.0 - 7.0 (sec)	0.83	correspond to 0.1g UBC S2 Spectra
Imperial Valley 1979 Brockman Road 230 degrees	4.95 - 9.95 (sec)	1.23	
Imperial Valley 1979 Brawley Airport 315 degrees	6.18 - 11.18 (sec)	1.08	correspond to 0.2g UBC S2 Spectra
Imperial Valley 1979 Pine Union School 140 degrees	8.15 - 13.1 (sec)	1.04	
Imperial Valley 1979 Imperial Valley College 140 degrees	4.0 - 9.0 (sec)	1.24	correspond to 0.4g UBC S2 Spectra
Imperial Valley 1979 Anderson Road 140 degrees	3.9 - 8.9 (sec)	1.15	

Rather than subjecting the test building to simulated earthquake motions from a single earthquake record, a series of "windows" from various earthquake records was recommended by Kariotis [12] to exercise the structure to increasingly severe behavior states. Three pairs of ground motions were selected corresponding to 0.1g, 0.2g, and 0.4g UBC S2 response spectra. These are presented in Table 1 with the selected time windows. The ground motions were scaled to match the UBC standard spectra within

certain ranges of periods. For motions with small v/a ratios, the range of period is selected from 0.6 seconds to 1.2 seconds, and for motions with large v/a ratios, the range of period is selected from 1.0 seconds to 2.0 seconds [12].

4 TEST DESCRIPTION

A total of 75 separate tests were conducted on the 5-story masonry research building over a period of approximately two months. Of these, 15 were GSD tests. In Figure 11, all the input ground motions used in the GSD tests are combined end-to-end to represent the complete record of the nearly 25 seconds of simulated seismic ground motion imposed on the research building. (Note that the building was exercised through additional cycles during the inverse triangular load tests conducted following each GSD test, but all primary damage to the structure was inflicted during simulated seismic motions.) In Figure 12, the acceleration, velocity, and displacement response spectra for four windows from the generated sequential acceleration record are presented for the case of 5% damping. The windows represent four target spectral response levels achieved during the tests: time 0-4 seconds approximating the 0.1g UBC S2 response spectra; time 0-13 seconds approximating the .3g level; time 0-21 seconds approximating the .4g level; and the entire record, time 0-25 seconds, approximating the equivalent of a .6g UBC S2 design response spectra.

A brief description of the key events, limit states, and response maxima for selected primary GSD tests follows, organized by the maximum building drift level attained. The term "drift" is defined here as the top floor lateral displacement divided by the building height. In the text, the direction of building displacement is related to the action of the hydraulic actuators: a positive displacement, with the long L-section wall flange in tension, corresponds to the "push" direction; a negative displacement, putting the long wall flange in compression, corresponds to the "pull" direction. Photographic records of the building damage are presented in Appendix A. The events are summarized in Table 2.

Maximum Drift: +0.020%, -0.016%

The first visible damage to the structure occurred at drift levels of +.010% and -.006%. The first cracks appeared in the construction joints between the cast-in-place slab topping (or footing) and the mortar joint at the base of the masonry walls on every floor level. Hairline cracks also appeared in the slab topping adjacent to the door on all floors. These cracks did not extend beyond the thickness of the masonry walls.

The first cracks in the long and short wall flanges, also at the construction joint between the foundation and the first mortar joint in the walls at the base, appeared at drift levels of +.020% and -.016%. The crack in the long wall flange was visible for 40 inches. The location and extent of all construction joint cracks was confirmed by rebar strain measurements and wall panel deformation and separation gages.

Maximum Drift: +0.030%, -0.026%

At this drift level, no new cracks opened in the masonry walls; behavior was characterized by continuing development of cracks that were initiated in previous tests. Cracks in the slab topping developed at every floor level in fan patterns with crack

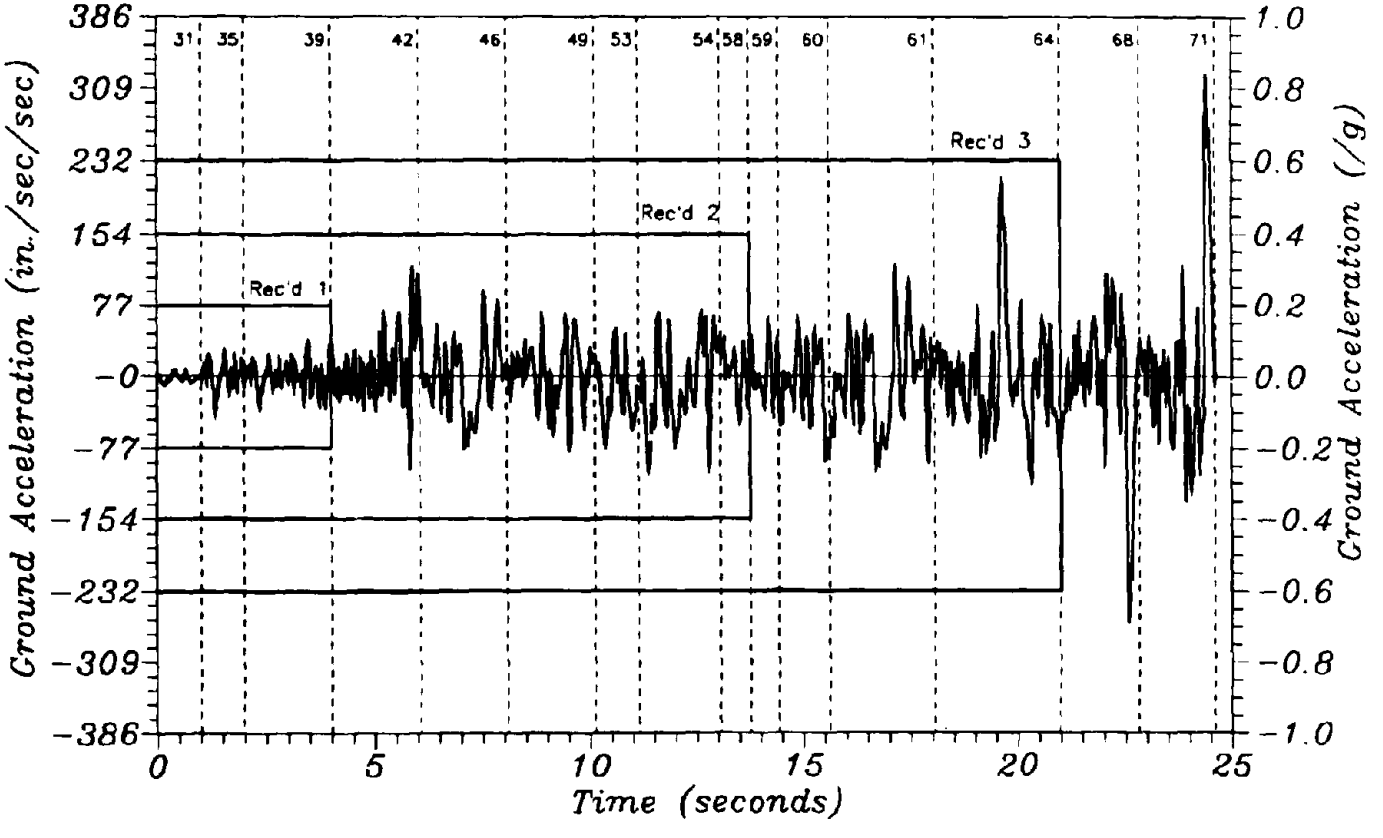

Figure 11 Generated Sequential Earthquake Record for 5-Story Building Test

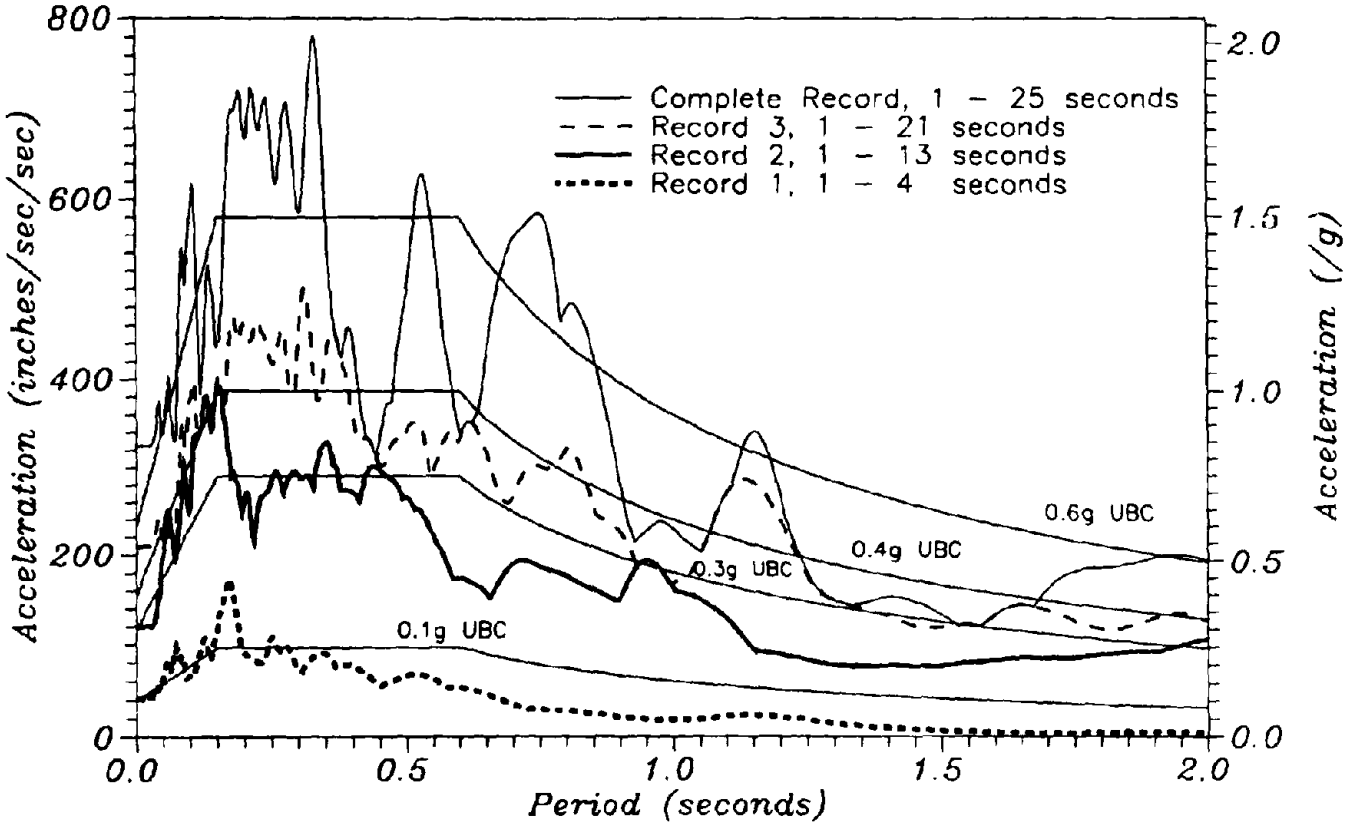

Figure 12 Acceleration Response Spectra (5% Damping) for Four Windows from the Generated Sequential Earthquake Record

lengths less than 12 inches. (The pattern of cracks is depicted in Figure A-8 for a greater drift level). No cracks were yet visible in the bottom of the precast planks.

Maximum Drift: +0.046%, -.0053%

First yield in the reinforcing was achieved in the long shear wall adjacent to the door at the level of the foundation/wall construction joint. Also, the first flexural cracks to develop in the walls (as opposed to the construction joints) were initiated in the bed joints of the long shear wall adjacent to the door.

At the maximum displacement levels, strain distributions in the vertical reinforcing in the flange walls in tension indicated that the short wall flange was under a nearly uniform strain of 750 μstrain, while the long wall flange showed a distinct shear lag effect, with strains of approximately 1700 μstrain at the wall intersection decreasing to near zero approximately 100 inches along the flange.

Maximum Drift: +0.068, -0.090

Full width flexural cracks appeared in the floor/wall construction joints of the long and short wall flanges at levels 1,2, and 3. Flexural cracks in the shear walls remained confined to the first three bedjoints above the foundation, adjacent to the door; cracks in the floor/wall construction joint extended across the entire length of both shear walls. Several short, diagonal cracks (less than 12 inches long) extended from the shear key locations at the base of the long shear wall, suggesting that a sliding mechanism developed, but was confined by the shear keys. Slip deformations at the base were of the order 0.01 inches.

In the slabs, the first cracks in the bottom of the precast planks developed in floors 1,2,3 and 4 (see Figure A-9). These cracks were typically less than 20 inches long and oriented diagonally. Cracks in the topping developed into a significant distribution of cracks in a fan pattern on both sides of the door, extending into the second plank (greater than 40") on floors 2,3, and 4, and remaining confined to the first plank in floors 1 and 5 (Figure A-8).

Strain gages indicated that the yielding zone at the base of the long wall extended to 5 bars on the adjacent to the door, and remained confined to one bar on the flange side. This is consistent with the predicted strain distribution for a flanged wall which would suggest a very small compression zone on the flanged side, and a larger zone on the opposite side when the flange steel is in tension. All bars in the long wall flange were activated, with a shear lag effect still evident. Four bars in the flange adjacent to the shear wall were yielding. Again, the short wall flange wall showed an essentially uniform strain distribution at approximately 1500 μstrain.

The long wall developed yield strains in the reinforcing adjacent to the door above the first story at the first floor.

Maximum Drift: +0.129%, -0.123%

The first cracks developed in the masonry of both long and short wall flanges. These cracks were nearly horizontal adjacent to the shear walls, but extended diagonally upward as they moved across the flange (Figure A-17c). At the same time, yielding across the entire width of both flanges developed at the foundation/wall construction joint. The strain distribution across both flanges was nearly uniform.

Horizontal flexure and diagonal flexural/shear cracks developed in both shear walls at the first story, and extend around the corner into the flanges. Yielding at the base extended to a zone of 2 bars on each side of the short wall, 5 bars at the door of the long wall, and 4 bars next to the flange.

Maximum Drift: +0.166%, -0.178%

Horizontal and diagonal flexural and flexure/shear cracks in the first story shear walls were well distributed, and the first flexural cracks in the masonry of the second story North wall appeared (Figure A-10a). Yielding in both shear walls extended across the entire base and up into the gage lines 32" and 64 inches above the foundation. The "plastic hinge" zone could therefore be considered to include the entire first story of the North longitudinal shear wall. Strains at the base of the long wall exceeded 8000 μstrain.

In the slabs, the first measured yielding occurred in the top of the lintel beam at floor 2, and at the bottom at floor 3.

Maximum Drift: +0.345%, -0.337%

Behavior at this drift level was characterized by the extension and development of existing mechanisms. New cracks continued to develop over the entire face of the first and second story, while strains in vertical reinforcing grew as high as 1.4% at the base of the long wall, and .9% in the short wall. Yielding was evident in top and bottom reinforcing in the slabs over the lintels, indicating the development of plastic hinges at floors 2,3, and 4.

Maximum Drift: +0.55%, -0.61%

Cracks continued to grow in the first story shear walls (Figure A-11), where very large strains (>2%) were measured in the vertical reinforcing bars. Diagonal flexure/shear cracks extended down almost to the corner of the long wall (Figure A-17c), indicating a very narrow flexural compression zone in the flange. The first indication of incipient crushing was apparent at the corner of the flange wall intersection in the long wall.

Flexural/diagonal cracks developed in the third story of the long shear wall along with yielding at the base of that wall (Figure A-17a). Strains in the vertical reinforcing in the long wall flange were nearly uniform at 3000 μstrain at the base. The fifth floor slab just achieved yield. First contact of a lintel with the adjacent wall was made at the first floor level (Figure A-12).

Maximum Drift: +1.00%, -1.44%

At the maximum negative displacement, vertical splitting occurred in the long wall at the flange (Figure A-13a) due to sliding of the first and second story walls (Figure A-13b). In the South wall, crushing of the flexural compression zone was evident, but not dramatic (Figure A-15b). The lintels at all floor levels made contact with the adjacent walls and immediately developed diagonal cracks with crushing at the corners (Figure A-18).

At a maximum displacement of +5.2 inches (+1.0% drift), a crushing failure occurred at the toe of the long shear wall (Figures A-14).

A selection of the key events described above are summarized in Table 2, and are related to the envelope of the base shear versus top floor displacement response in Figure 13.

Table 2 Record of Key Events

	Event	Test No.	Drift (%)	Top Displ.
1	First crack in floor/wall construction joint adjacent to door in the long and short shear walls (Floors 0,1,2,3,4)	031	+.010 -.006	+.052 -.030
2	First crack in slab topping, adjacent to door (Floors 1+,2-,3+,4,5)	031	+.010 -.006	+.052 -.030
3	First crack in floor/wall construction joint in long and short wall flanges. (Floor 0)	035	+.020 -.006	+.105 -.082
4	Development of slab topping cracks in fan pattern < 12" (Floors 2-,3-,4-)	039	-.026	+.133
5	First flexural cracks in mortar joints of shear walls (Floor 1)	042	-.054	-.277
6	First yield in long wall adjacent to door	042	-.054	-.277
7	First crack in bottom of precast plank (Floors 1+,2-,3+,4+-)	046	+.070 -.092	+.359 -.474
8	Development of cracks in floor/wall construction joints in both flanges (Floors 2,3,4)	046	+.070 -.092	+.359 -.474
9	Yield in long wall flange at base (4 bars)	046	+.070	+.359
10	Yield in long wall at Floor 1 adjacent to door	046	-.092	-.474
11	First crack in masonry of both flanges.	049	+.13 -.12	+.665 -.633
12	Yielding across entire width of both flanges at base.	049	+.13 -.12	+.665 -.633
13	First yield in slabs in pull direction: Floor 2 top, Floor 3, bottom	054	-.18	-.917
14	First cracks in second story long wall	054	+.17 -.18	+.854 -.917
15	Yield in slabs: Floors 2,3,4	061	-.22	-1.15
16	Vertical bars in first story yield up to 64" above base	064	+.35 -.34	+1.78 -1.74
17	Flexural cracks develop in 3rd story wall	068	-.61	3.15
18	Vertical splitting of long wall, and sliding of first and second story walls	071	-1.45	-7.5
19	Crushing of lintels on all floors	071	-1.45	-7.5
20	Crushing at toe of long wall adjacent to door, at base and floor 1, short wall at base.	071	+1.0	+5.2

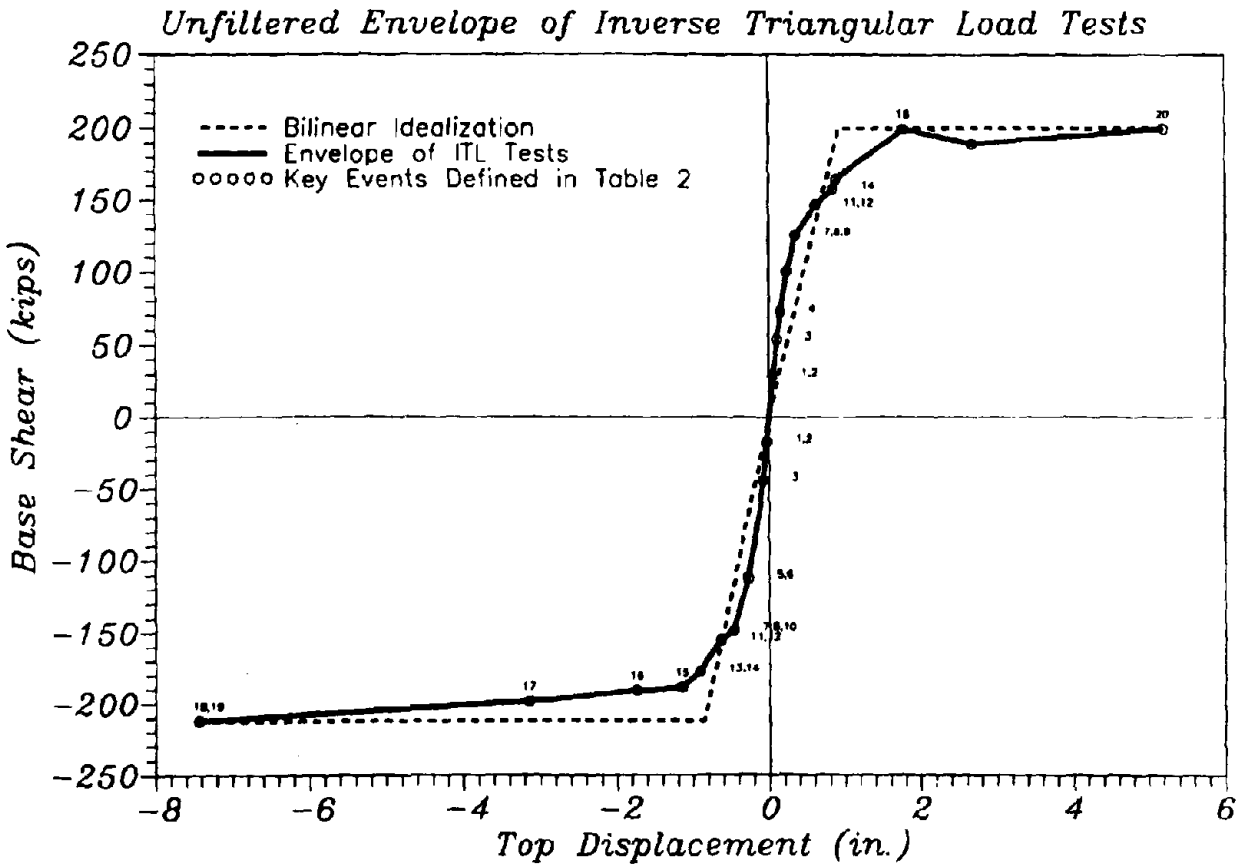

Figure 13 Key Events from Table 2 Related to Envelope of the Base Shear vs. Top Displacement Response from Inverse Triangular Tests

5 SUMMARY AND ANALYSIS OF TEST RESULTS

For the purpose of this preliminary report, characteristic test results will be presented first to demonstrate the GSD procedure and the associated experimental measurements. Second, a typical test sequence comprised of a GSD test, an Inverse Triangular Load test, and a Modal Stiffness measurement will be described. Finally, the overall performance of the 5-story research building will be evaluated by presenting the base shear versus top floor displacement response, since this corresponds directly to the predicted response used in the pre-test analysis and design models (see section 2). In the final report on the 5-story building test, a complete documentation of all pertinent data recorded during each test sequence will be provided.

5.1 Description of a Typical GSD Test

An example of typical GSD test results from a low-level test (Test 016), is presented in Figure 14, showing the floor displacement history for each of the five floor levels, the floor load time history, and the displacement error time history. Test 016 represents a successful application of the GSD test method to the stiff, uncracked structure as part of the systems shakedown tests before the generated earthquake input sequence in Figure 11 was initiated.

The predominantly first mode response can be seen in the floor displacement time history in Figure 14(a), while Figure 14(b) depicts higher mode oscillations in the measured restoring force response. These higher mode characteristics are also evident in the displacement error time history, see Figure 14(c). However, it should be noted that both the displacement error and the magnitude of the spurious higher mode restoring force contributions could be tightly controlled, i.e. in the example of Test 016 to approximately 0.0005 inches of displacement and approximately 2 kips of restoring force, which is quite remarkable for stiff multi-degree of freedom shear wall structures.

5.2 Description of a Representative Test Sequence

Basic results from a typical three-test sequence, at a displacement ductility level near μ=1, are shown for Test 061 in Figures 15-17. Figure 15 shows the input ground acceleration record along with the corresponding recorded floor displacement and restoring force time histories. The GSD segment for Test 061 was a 2.45 second window for the Brawley Airport earthquake record recorded during the 1979 Imperial Valley (M_s=6.8) earthquake. The record was scaled by a factor of -1.4 to produce target building top displacements of +1.3 inches (push) and -1.4 inches (pull). Predictions of the building response were performed using linear elastic implicit time integration schemes with a time step of 0.01 seconds, based on the experimentally obtained modal stiffness matrix just prior to the GSD test segment. As can be seen from Figure 15, the building response was again predominantly first mode, with spurious higher modes of controlled magnitude appearing in the restoring force record. It should be pointed out here that no artificial numerical damping was employed to control spurious higher mode effects during the GSD tests. The actual achieved maximum response displacements of push +0.88 inches and pull -1.15 inches show how difficult it was at this structural limit state to predict the actual

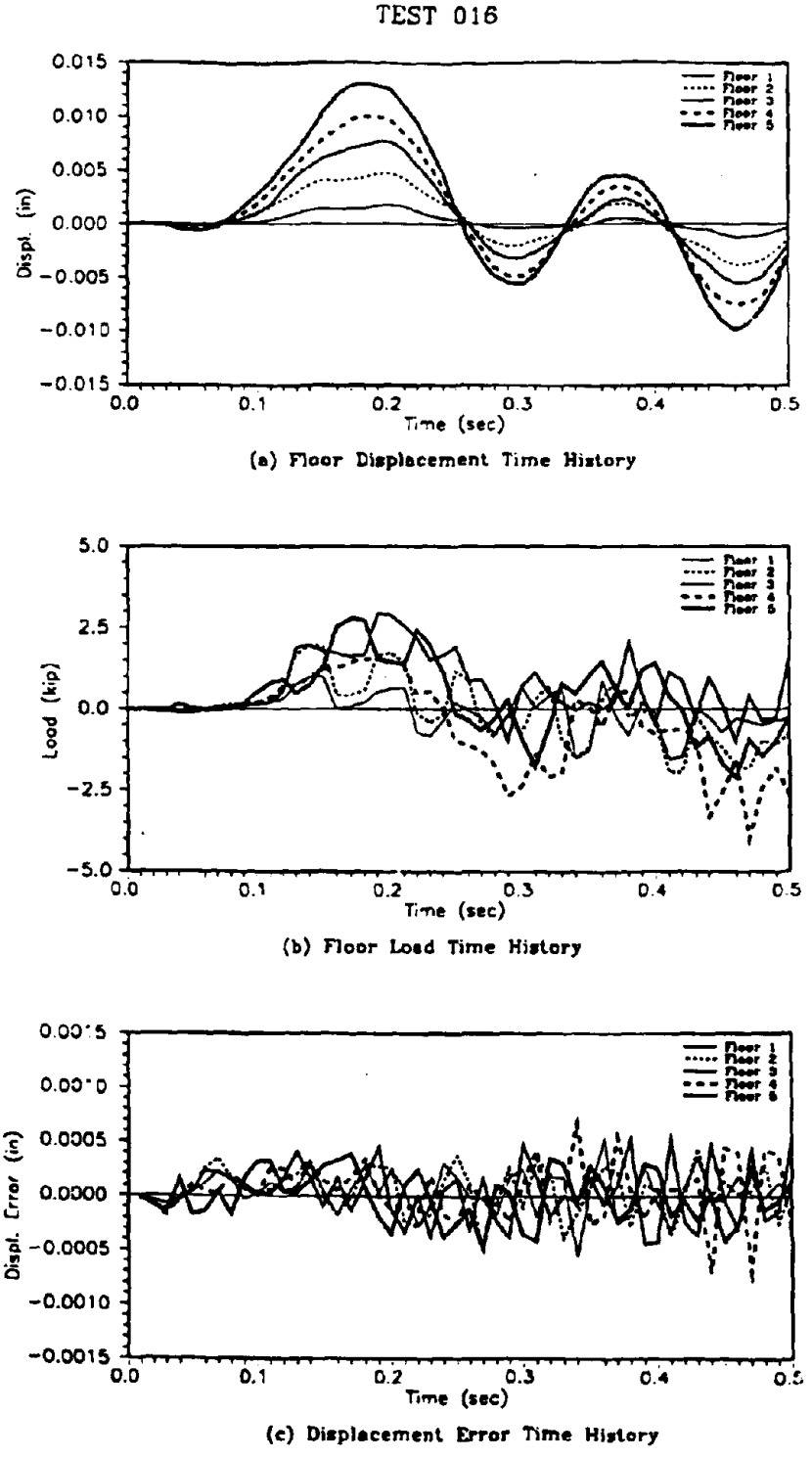

Figure 14 Typical Low-Level GSD Test Results

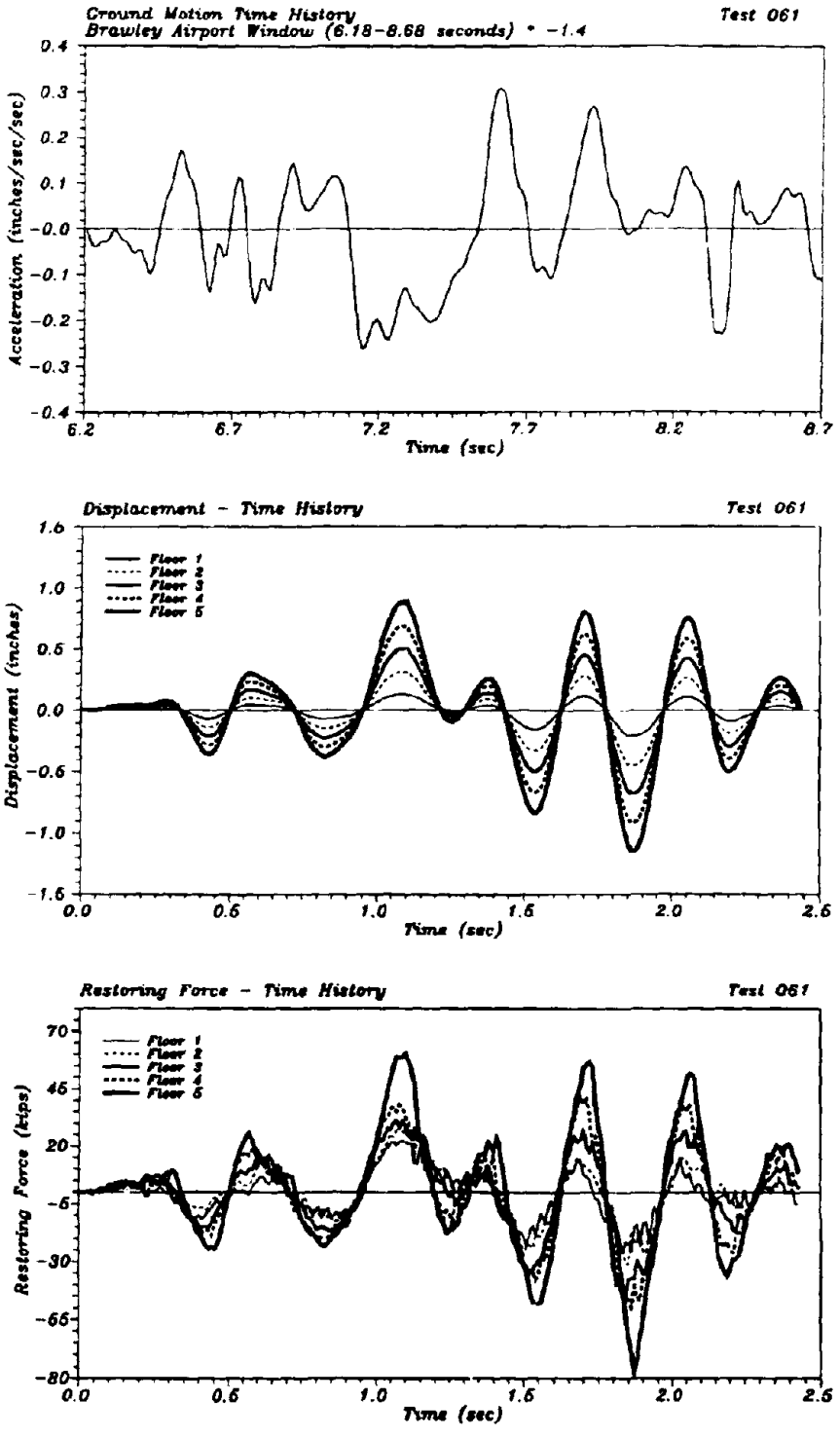

Figure 15 Typical GSD Test Results Near Displacement Ductility 1

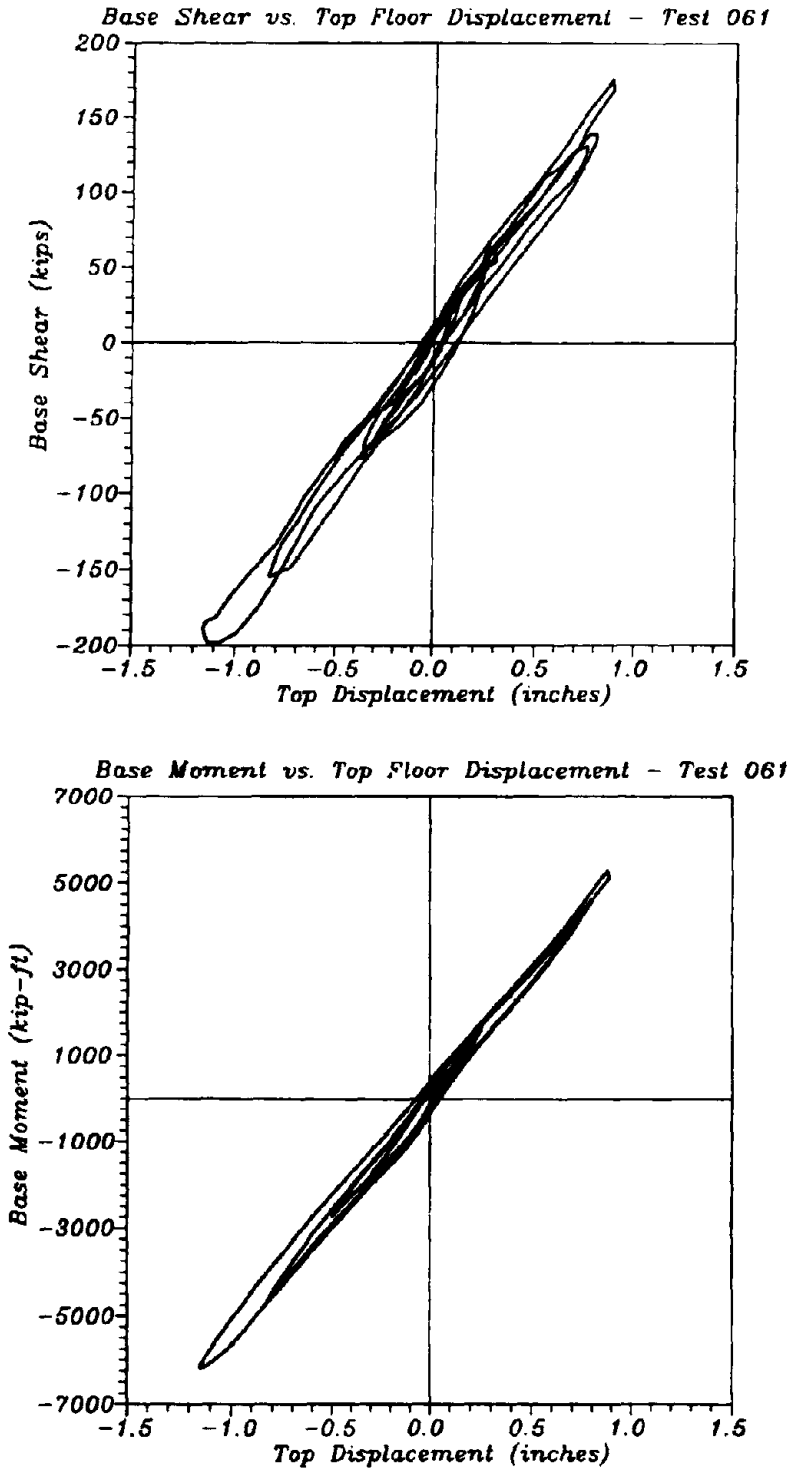

Figure 16 Typical (a) Base Shear and (b) Base Moment vs. Top Displacement Response from a GSD Test

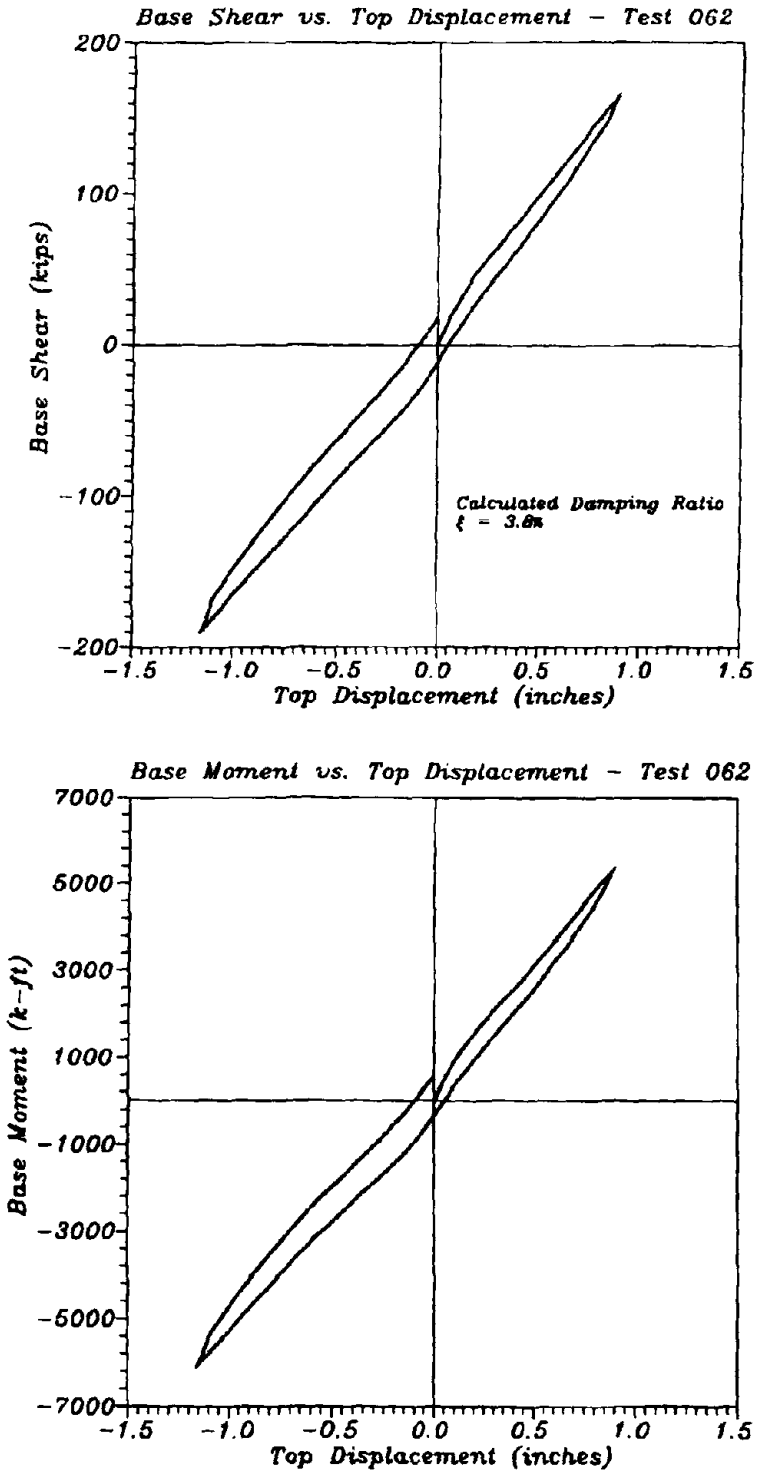

Figure 17 Typical (a) Base Shear and (b) Base Moment vs. Top Displacement Response from ITL Test

displacement levels using linear elastic time history extrapolations. During each GSD test, base shear vs. top floor displacements and base moment vs. top floor displacement were monitored in real time, as depicted in Figure 16. The smooth, well-behaved cycles illustrated in both plots indicate successful performance of the structure in terms of stable hysteresis characteristics with no stiffness degradation. Each GSD test was followed by a single-cycle ITL test up to the previously achieved maximum displacement levels such as the one illustrated in Figure 17 for test 062. Here again, base shear and base moment versus top floor displacement is shown. The ITL tests allowed an accurate calculation of the current level of the hysteretic damping, in this case having a value of 3.8%. In addition to the GSD and ITL tests, but not shown here, each test included a modal stiffness measurement for the complete characterization of the building condition.

5.3 Overall Building Response

The response of the building is represented in Figure 18 by the superposition of all of the individual GSD tests, which may be loosely interpreted as the response of the structure to the entire ground motion illustrated in Figure 11. The thick dotted line indicates the overall load-displacement envelope of these tests. Similarly, the superposition of all ITL tests is presented in Figure 19 with a thick solid line indicating the envelope of the response. The last GSD test did not constitute a full cycle, as it was terminated after actuator limits in the maximum negative or pull direction were reached. The test was completed by a final cycle in the push direction to the target displacement of 1% drift or 5.2 inches in an ITL mode. Since the final, positive displacement portion of the cycle was carried out under an inverse triangular load distribution, it is only presented in Figure 19 together with the other ITL tests.

A comparison of the GSD and ITL envelopes is presented in Figure 20(a). The total base shear developed in the GSD tests is approximately 30% greater than that in the ITL tests, particularly in the pull direction, with the long wall flange in compression. Similar response would have been expected in the push direction had the GSD test been carried to completion. The difference in the measured response from the two tests may be explained in part by strength degredation between cycles, although past experience suggests that this would account for a drop of less than 5%. A greater part of the difference may be attributed to the amplification of base shear that occurs due to higher mode effects. This is illustrated in Figures 20(b), (c), and (d) which represent the same data modified by the use of a simple "data filter". In order to understand the nature of data filter, first consider the distribution of loads on a structure undergoing pure, first mode response. The load distribution approximates an inverted triangle, with a resultant force located near 2/3 of the building height. In the case of the 5-story test building, the actual location of this resultant is 0.72h, or 31'-2" up from the base. Any deviation of the lateral force resultant from this location suggests the presence of higher mode force distributions. In the data filter, the force distribution at each load step of both GSD and ITL tests was evaluated, and the location of the resultant compared to the ideal first mode location. Data that failed to match the first mode resultant location, within a specified error tolerance, was discarded. The curves in Figures 20(b), (c), and (d) represent the results of this data filter for three successively smaller error tolerances:±20, ±10, and ±5 inches respectively. It can be seen that as data representing the higher mode

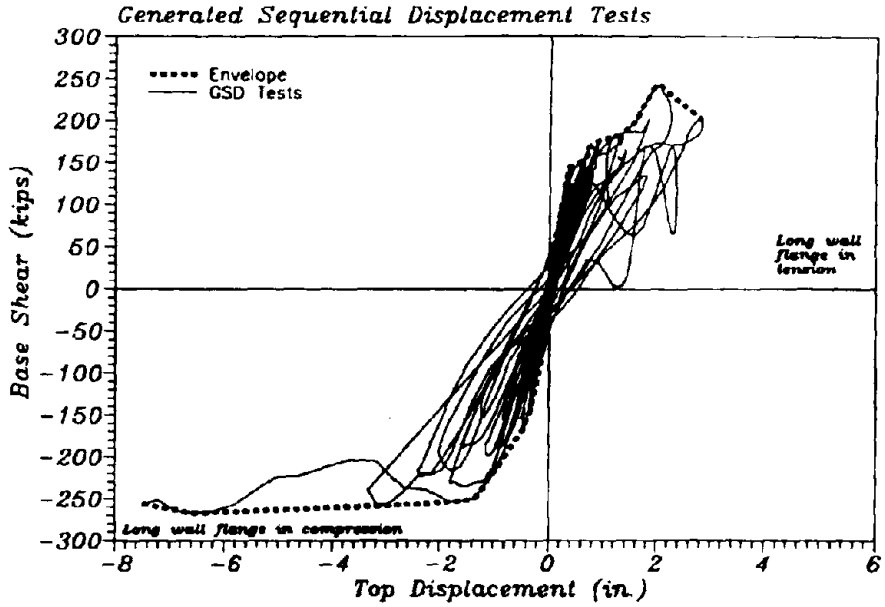

Figure 18 Combined Base Shear vs. Top Displacement Response from GSD Tests

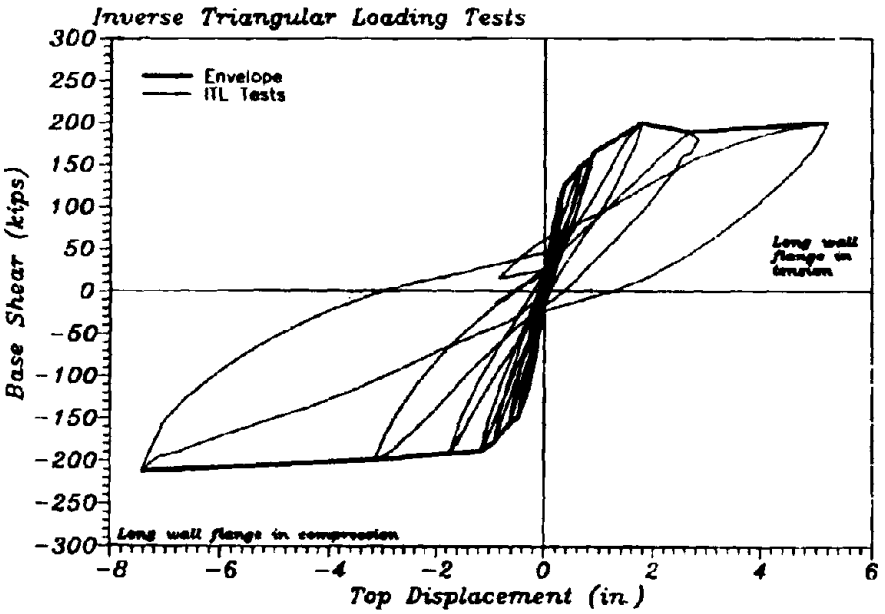

Figure 19 Combined Base Shear vs. Top Displacement Response from ITL Tests

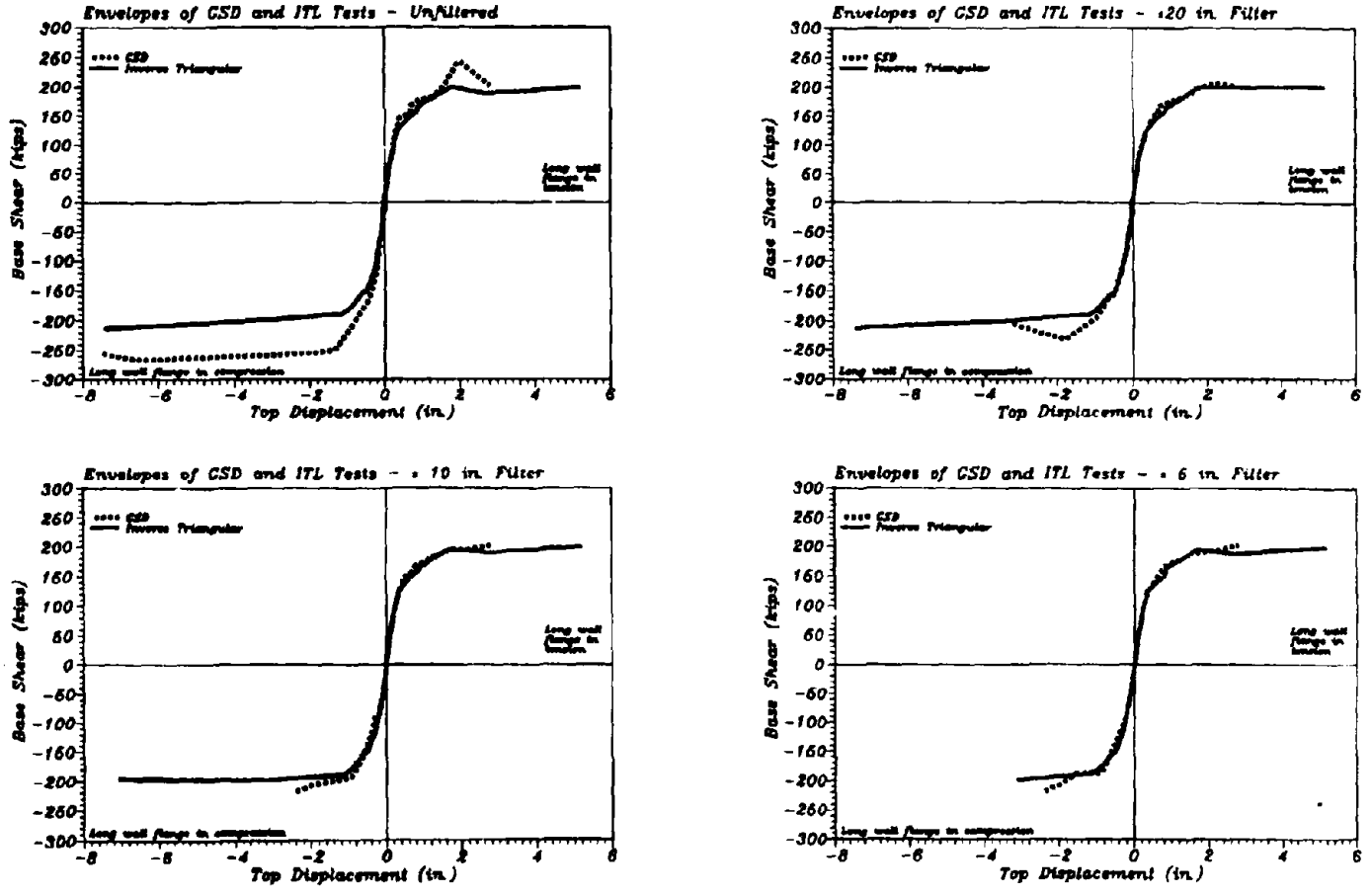

Figure 20 Comparison of Envelopes from GSD and ITL Tests for (a) Unfiltered data (b) Data filtered to ±20 inches, (c) ±10 inches, and (d) ±5 inches

force patterns was discarded, the response of the GSD tests agreed more closely with that of the ITL tests. It is also clear, as might be expected, that the ITL test envelope was less severely affected by the filter, since the applied force distribution already approximated the first mode distribution of forces.

The difference in the base shear developed in the GSD and ITL tests illustrates the necessity, in the capacity design approach, of applying a dynamic amplification factor (see section 2 and reference [6]), to the base shear values calculated for first mode force distributions. The shear developed in the test building was greater by a factor of 1.3 under simulated seismic forces than under ideal inverse triangular force distributions. This may be compared to a higher mode amplification factor used in the design of 1.4.

The unfiltered envelope of inverse triangular load tests are compared in Figure 21 with the idealized bilinear representation of the piecewise linear response prediction used for design, and the nonlinear finite element prediction. The design base shear level is also shown as a horizontal dashed line extending to a displacement 4.5 times the predicted yield displacement.

A comparison of the experimentally measured initial stiffness in Figure 21 with that predicted by the analytical models shows that the finite element model provided an excellent prediction of initial stiffness of the structure. This idealized bilinear design model clearly features a lower initial stiffness since the design model sought to characterize the behavior of the structure at some intermediate point between the initial, extremely stiff, uncracked state, and the final condition of the structure in which yield mechanisms have developed in the walls and slabs. This point is further exemplified by a comparison of predicted and experimentally measured periods of vibration shown in Table 3. The predicted vibration periods are based on the FEM model for the initial uncracked state, and the simple, linear beam element model of the yield limit state. Agreement between the predictions and the test results is acceptable in both cases, particularly for the first (primary) mode of response.

Table 3 Comparison of Predicted and Measured Periods of Vibration

Mode	Period (seconds)			
	Walls and slabs uncracked		Walls and slabs yielded	
	Predicted (FEM)	Measured	Predicted (Linear Beam)	Measured
1	0.203	.208	.490	.523
2	0.053	.057	.069	.112
3	0.026	.026	.025	.039
4	0.019	.019	.014	.028
5	0.016	.016	.008	.018

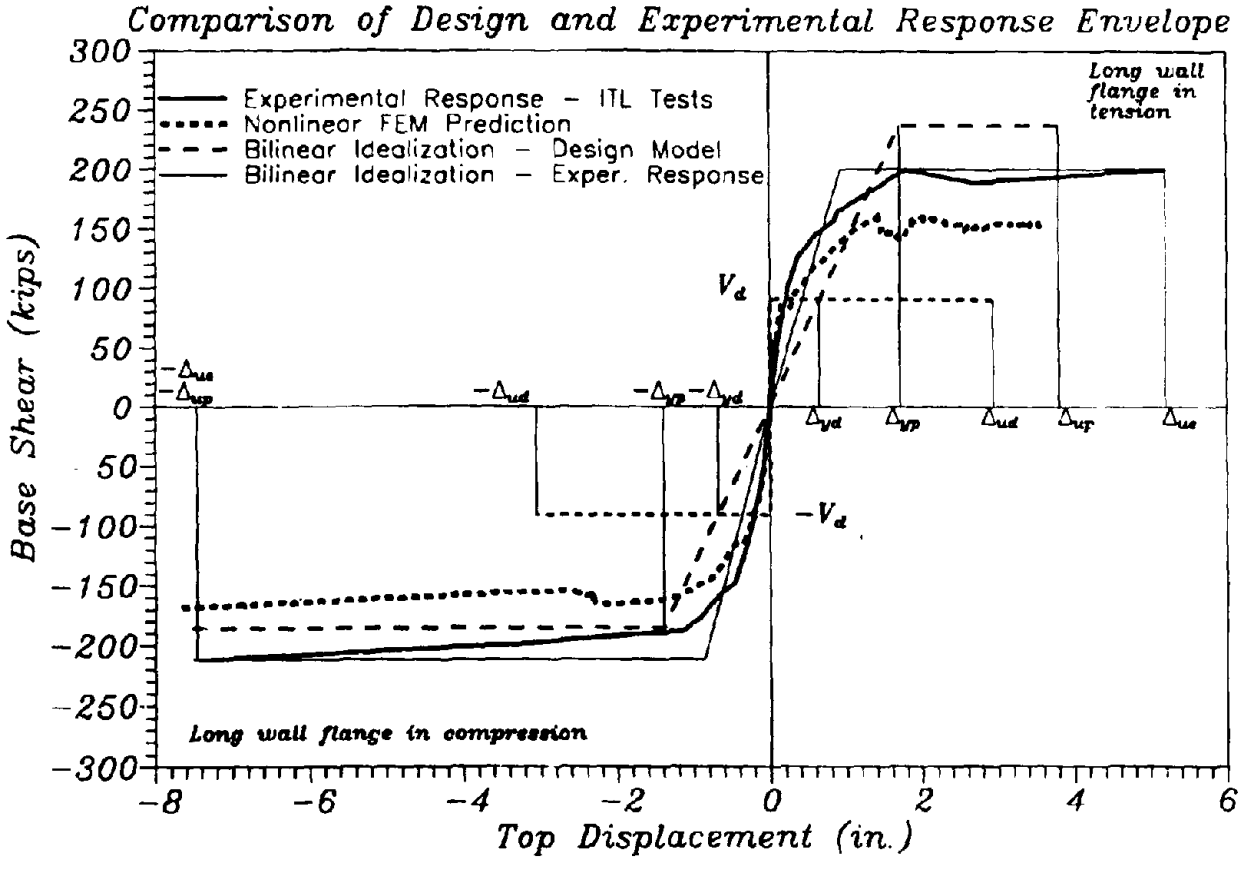

Figure 21 Comparison of Predicted and Experimental Response Envelopes

The displacement ductility achieved in the test building is illustrated in Figure 21. The measured performance ductility of the structure was greater than 6 in the push direction when the long wall flange was in tension, and greater than 9 in the pull direction with the long wall flange in compression. Comparison of these values to the predicted values (shown in Figure 8) of 2.2 and 5.4, respectively, or to the stipulated design value of 4.5, illustrates the exemplary performance of the test structure.

In terms of ultimate load capacity, the analytical models provided satisfactory predictions in the pull direction (long wall flange in compression), with the finite element model underestimating the total capacity. Predictions of ultimate displacement were excellent for both models. This is consistent with the purely flexural response mode of the structure when loaded in this direction. In the push direction, (long wall flange in tension), both models underestimate the ultimate displacement, and the design model overestimated the ultimate strength, while the finite element model again underestimated the strength. In this loading direction, the simple design model was most sensitive to the parameters of effective slab width and effective flange width, and to the assumption that the shear walls can be idealized by a line element located at the elastic neutral axis of the section. Additional analysis of the data will be required to make improvements to the model. In the finite element model, underestimation of the strength in both directions suggests an under-prediction of the coupling contribution to the lateral load resistance. A limited amount of coupling can be attributed to the loading beams which were instrumented at later test stages to quantify this effect. Post-test parameter studies with the FEM model included the load beams, and show an increase in the analytical capacity levels close to those experienced during the test.

In the final report, the additional coupling effects of the load beams, estimated currently at approximately 10% of the total base shear, will have to be accounted for both in the actual behavior of the test building and in the final analytical modeling.

The progressive development of a plastic hinge mechanism in the test structure agreed quite well with the mechanism sought in the design (see Section 2 and Reference [6]). Stable, ductile flexural hinges developed in each of the five floor slabs in the door region between the two shear walls, with no evidence of brittle failure in the slabs even at rotations up to three times the overall building drift. Brittle failure of the nonstructural lintels did not occur until the building attained an overall drift level of -1.4% (see Figure A-18). Flexural hinges developed at the base of both shear walls, with deformations distributed over numerous horizontal and diagonal cracks extending throughout the first two stories and into the third story walls (see Figure A-17). Measured strains indicated yielding in the vertical reinforcing bars as high as the base of the third story wall. In the flange walls, preliminary analysis of observed cracks and measured strains confirmed the design values for effective width in these walls. The development of distributed cracks in both flanges (Figure A-17) further confirmed the development of ductile yield mechanisms due to effective reinforcement design.

6 CONCLUSIONS

The successful completion of the first U.S. 5-story full scale building test under simulated seismic loads has provided new milestones in terms of structural systems testing not just in the U.S., but world wide. For the first time, a stiff shear wall type 5-story structure was tested from beginning to end utilizing simulated seismic load input and not any predetermined fixed lateral load patterns.

For the U.S. TCCMAR program, the 5-story full scale reinforced masonry building test provided key validations for both, design models and analytical predictive tools. The test demonstrated that masonry buildings in seismic zones can be designed with ductile performance characteristics with achieved test ductilities of approximately 6 and 9 in the push and pull directions respectively. These achieved displacement ductility levels by far exceed required design ductilities and even the estimated predictions, without any loss of lateral load carrying capacity. Load-deformation hysteresis loops were stable to the end of the test and showed hysteretic energy absorption equivalent to 13.3% of critical viscous damping for the final cycle.

Inelastic structural action was predominantly limited to the design location of first story walls, with inelastic flexural action extending to the base of the second and third story walls at the final test stage. TCCMAR design guidelines on the amount and distribution of both vertical and horizontal reinforcement resulted in well distributed flexural and flexural/shear crack patterns. Crack patterns in the wall flanges and reinforcement strains showed that the entire flange width was effective; strain measurements and crack extensions in the floor slabs will allow for a detailed post-test evaluation of the effective width at various design limit states. The decoupled doorway lintel design proved very successful, with no damage up to overall building drift levels of 0.5%, and only minor damage with no significant lateral capacity increase at higher deformation levels. Thus, for moderate seismic excitations, no visible damage of a masonry building designed based on the new TCCMAR design criteria can be expected.

Finally, the 5-story research building test provided invaluable benchmark data for the verification and calibration of predictive analytical models in support of seismic building design and assessment.

The intent of this preliminary report was to provide a first overview of the 5-story full-scale U.S.-TCCMAR research building test. Detailed descriptions of the employed GSD test procedure, the predictive and diagnostic analytical model development, a detailed presentation of all experimental data, and a summary of behavior data in direct comparison with analysis and design models will be presented in a comprehensive final test report.

REFERENCES

1. NEHRP Recommenced Provisions for the Development of Seismic Regulations for New Buildings, Part 1 - Provisions, Federal Emergency Management Agency (FEMA), October 1988.

2. NEHRP Recommenced Provisions for the Development of Seismic Regulations for New Buildings, Part 2 - Commentary, Federal Emergency Management Agency (FEMA), October 1988.

3. Proposal 5-1 for the addition of a new appendix to Chapter 12, Masonry, in the NEHRP Recommenced Provisions for the Development of Seismic Regulations for New Buildings, Part 1 - Provisions, Jan 1991.

4. Proposal 5-1 for the addition of a new section to the end of the commentary to Chapter 12, Masonry, in the NEHRP Recommenced Provisions for the Development of Seismic Regulations for New Buildings, Part 2 - Commentary, Jan 1991.

5. Paulay,T., and Priestley, M.J.N., "The Stability of Ductile Structural Walls," Proposed addition to the appendix to Chapter 12, Masonry, in the NEHRP Recommenced Provisions for the Development of Seismic Regulations for New Buildings, Part 1 - Provisions, Jan 1991.

6. Seible, F., Priestley, M.J.N., Hegemier, G.A., Kingsley, G.R., Igarashi, A., Kurkchubasche, A.G., "The Test Plan for the 5-Story Full-Scale TCCMAR Research Building," Structural Systems Research Project, Report No. SSRP-91/07, UCSD, November 1991.

7. Paulay T., and Priestley, M.J.N, Seismic Design of Reinforced Concrete and Masonry Structures, John Wiley and Sons, 1992.

8. Seible, F., Priestley, M.J.N., Kingsley, G.R., and Kurkchubashe, A., "Flexural coupling of Topped Hollow Core Plank Floor Systems in Shear Wall Structures", Structural Systems Research Project, Report No. SSRP-91/10, UCSD, December 1991.

9. Priestley, M.J.N, and Limin, H., "Seismic Response of T-Section Masonry Shear Walls," The Masonry Society Journal Vol. 9, No. 1, August 1990, pp. 10-19.

10. Priestley, M.J.N, and Hart, G.C., "Design Recommendations for the Period of Vibration of Masonry Wall Buildings," Structural Systems Research Project, Report No. SSRP-89/05, UCSD, November 1989.

11. Seible, F., and Igarashi, A., "Full Scale Testing of Masonry Structures Under Simulated Seismic Loadings," Experimental and Numerical Methods in Earthquake Engineering, (Donea, J. and Jones, P.M. ed.), 1991, pp.119-148.

12. Kariotis, J.C., Personal Correspondence to F. Seible, August 8, 1991.

ACKNOWLEDGEMENTS

A large experimental test such as the one described in this preliminary report can only be successful through the collaboration, support, and help of many dedicated individuals, agencies, and industry groups.

This first 5-story full scale seismic building test in the U.S. was made possible by several research grants from the National Science Foundation, and funds from the Department of Energy. Support was also provided by the masonry industry, in particular the Masonry Institute of American and the Masonry Association of California and Nevada. The project was generously supported by Blocklite which provided the masonry units, and Spancrete which provided the precast hollow-core planks. H.G. Fenton donated all the premixed concrete for grout and topping. Dywidag Systems International provided the post-tensioning hardware, and Martin Marietta the liaison to the Department of Energy.

The program was carried from its design and development stage to the final test by the support of the TCCMAR group of researchers, too numerous to name here, who contributed invaluably to the success of the test with their suggestions and constructive criticisms.

Individuals who deserve special appreciation for their contributions are Dr. Jack Scalzi, Program Director NSF, who initiated the TCCMAR project and had the vision to push for and provide the first U.S. 50-foot reaction wall facility, Dr. Chi Liu, Program Director NSF, under who's guidance the 5-story test was performed, and Dr. James L. Noland of Atkinson-Noland and Associates, who coordinated the TCCMAR program.

Finally, the success of the test was due in large measure to the professional and dedicated service of the entire staff and support crew of the Charles Lee Powell Structural Systems Laboratory.

APPENDIX - A

Photo Documentation of the 5-Story Full Scale Reinforced Masonry Research Building Test

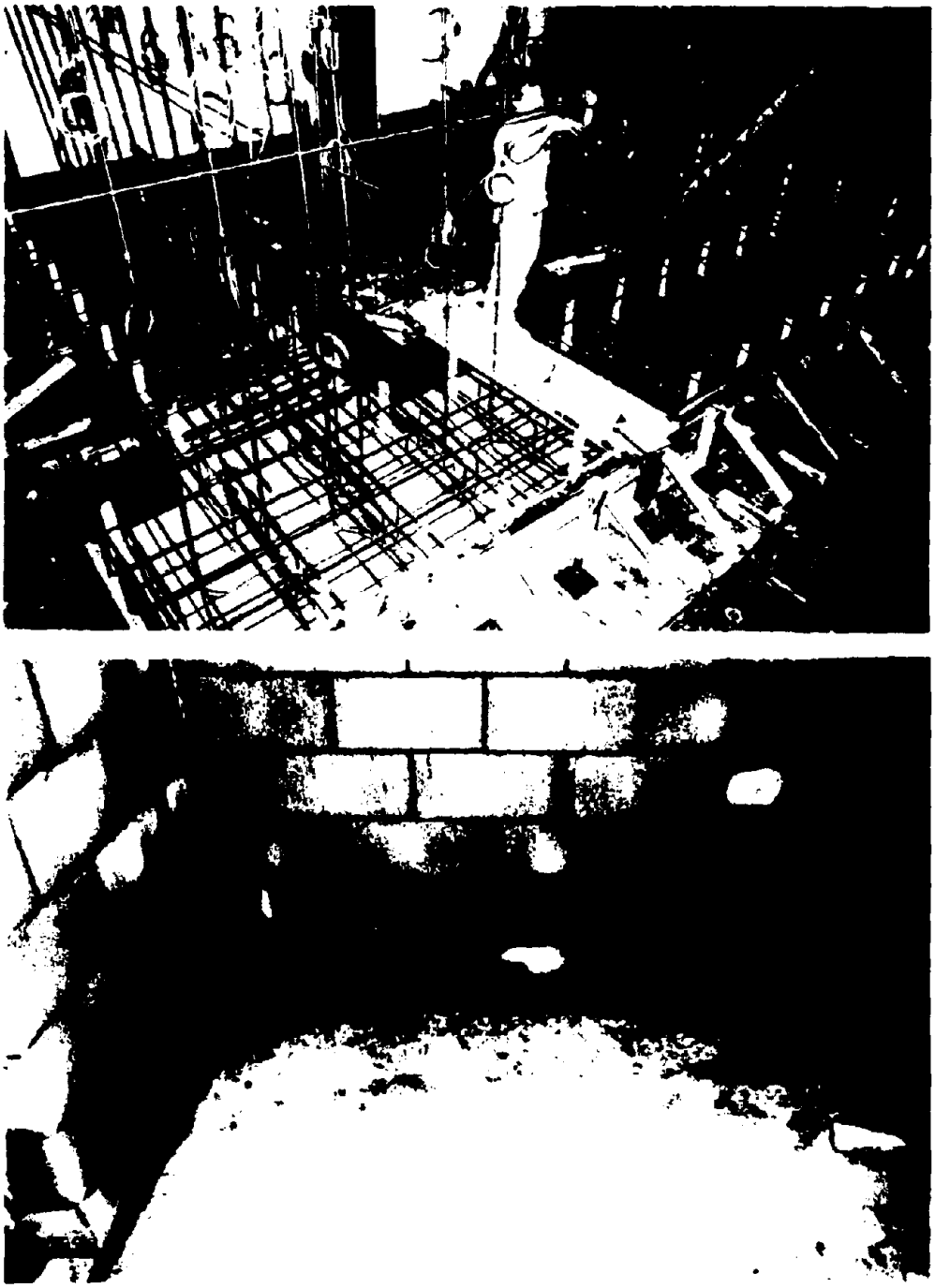

Figure A 1 Construction of Footing and Masonry Wall Cleanout Detail

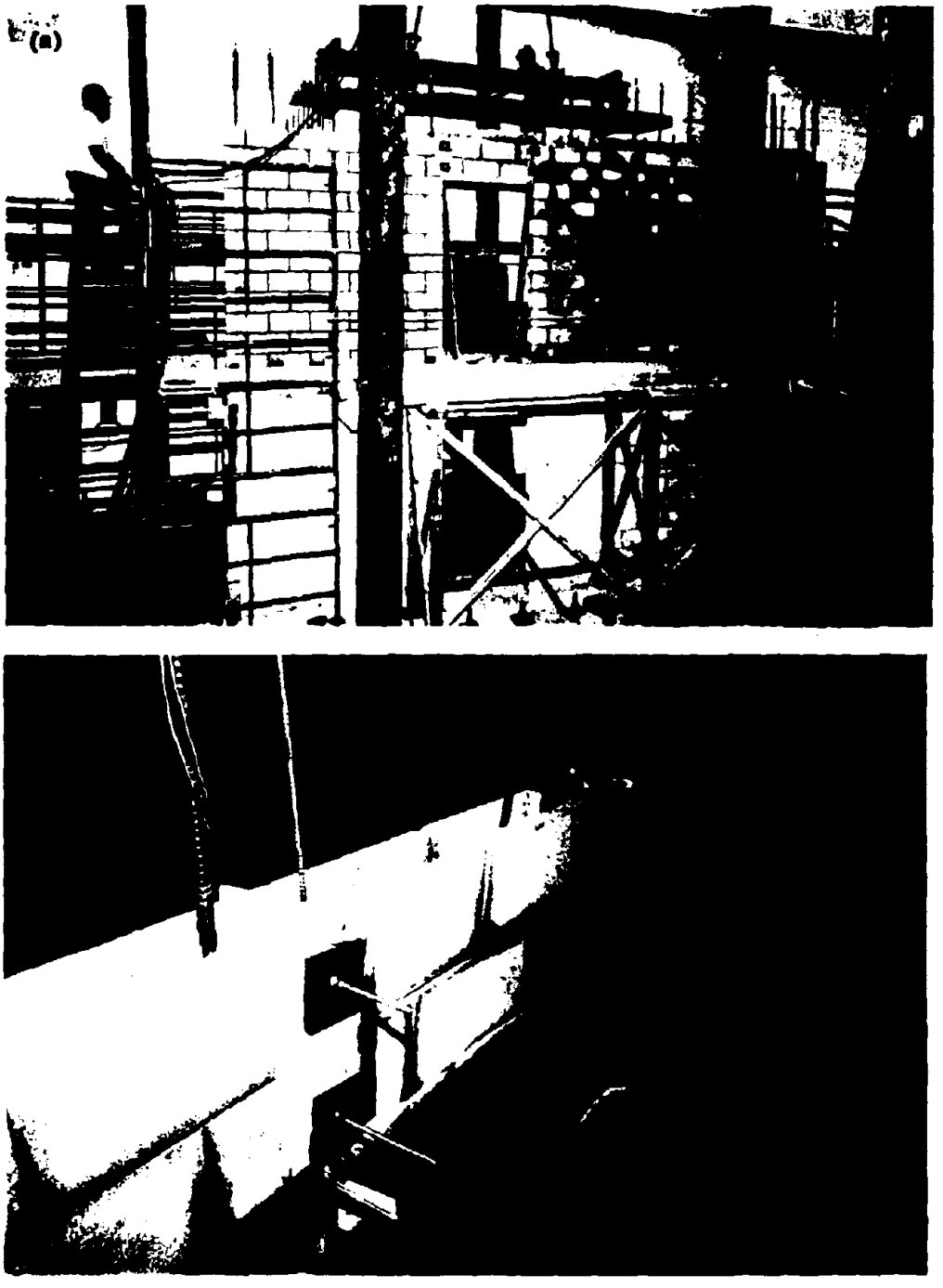

Figure A-2 Placement of 2nd Floor Planks and Lintel Detail Prior to Grouting

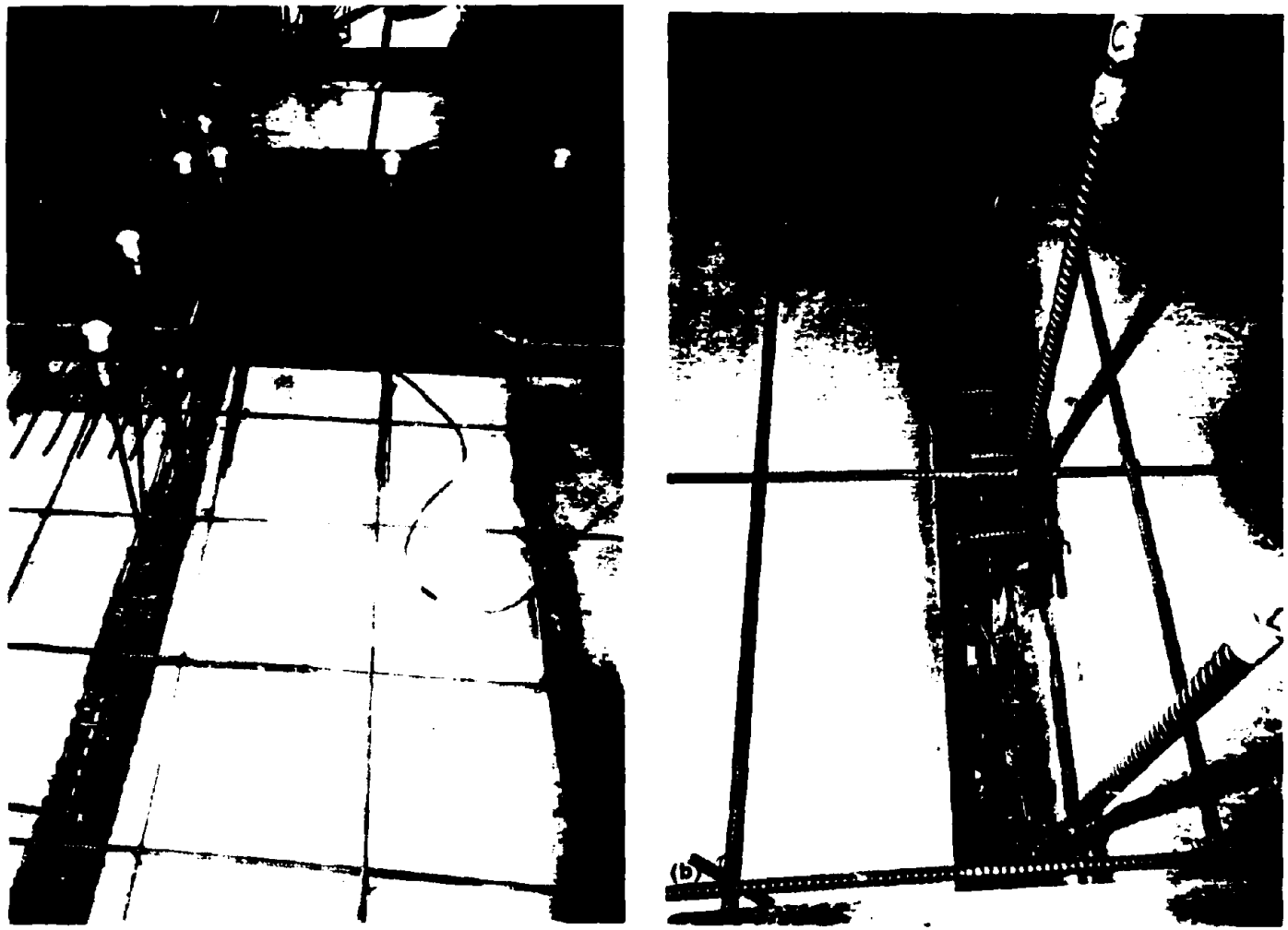

Figure A-3 Integral Lintel Beam and Topping Reinforcement

Figure A-4 Completed 5-Story RM Research Building and Actuator System

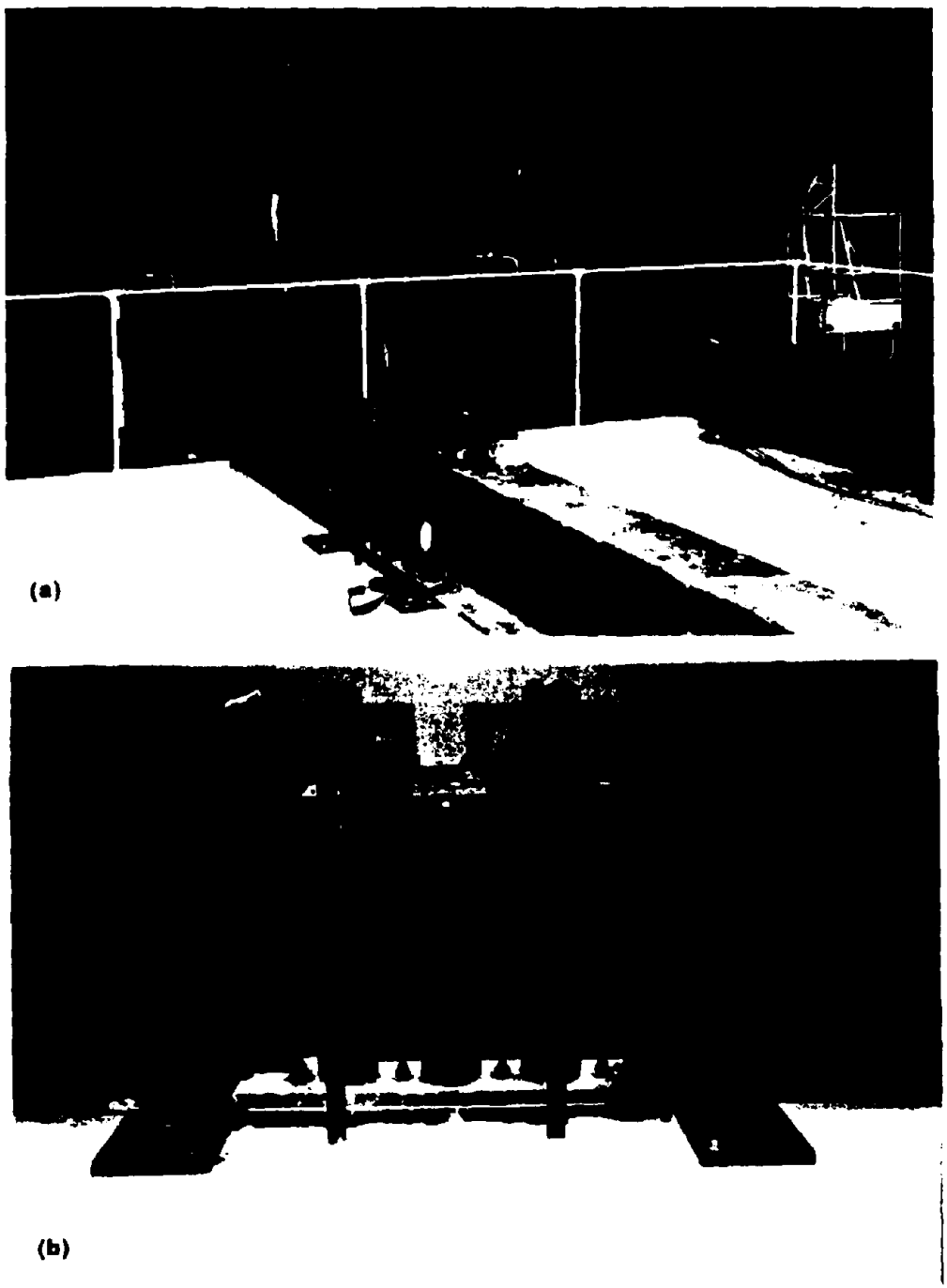

Figure A-5 Load Beams and Connection to Floor System

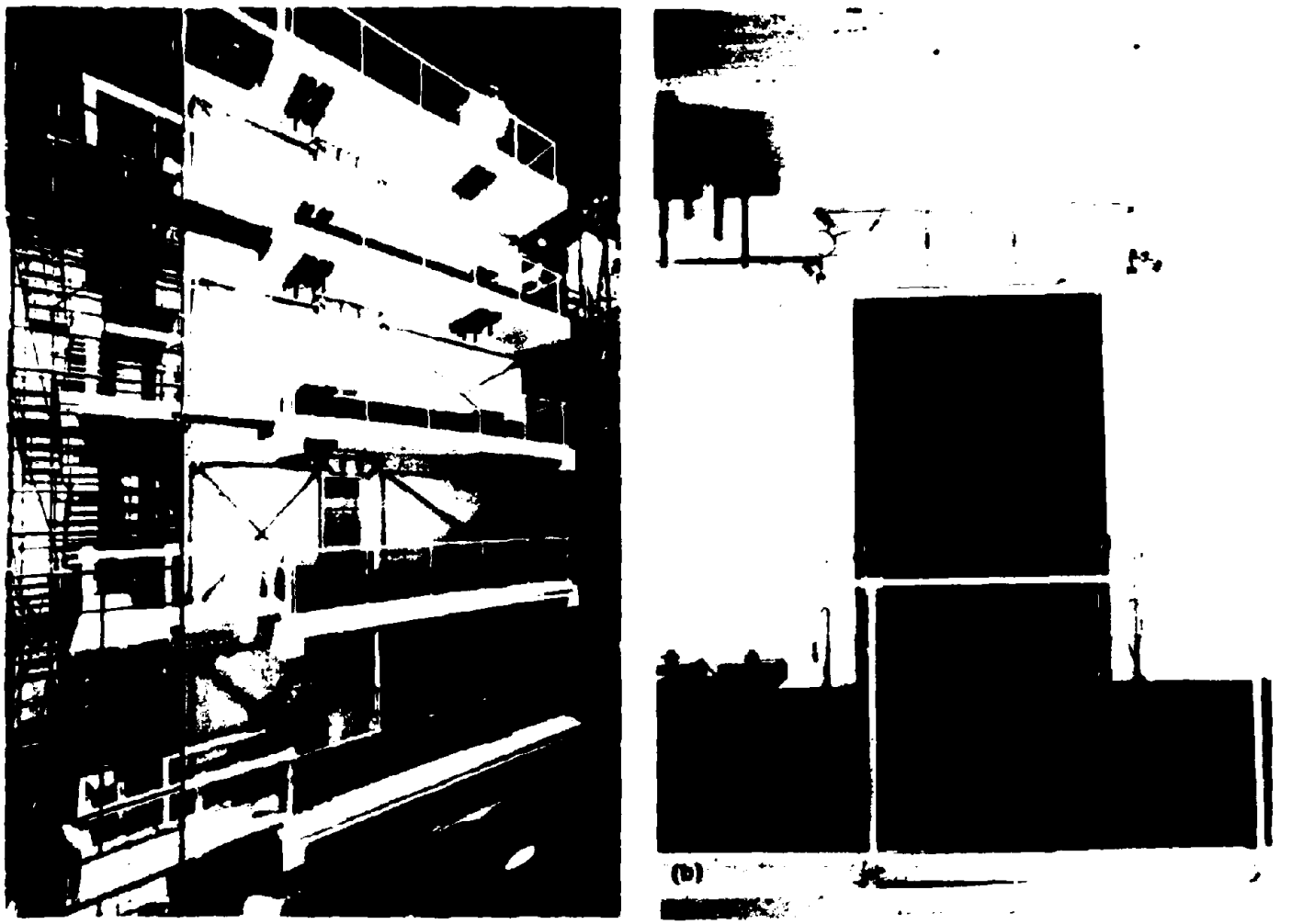

Figure A-6 Instrumentation Overview and Lintel Rotation Instrumentation

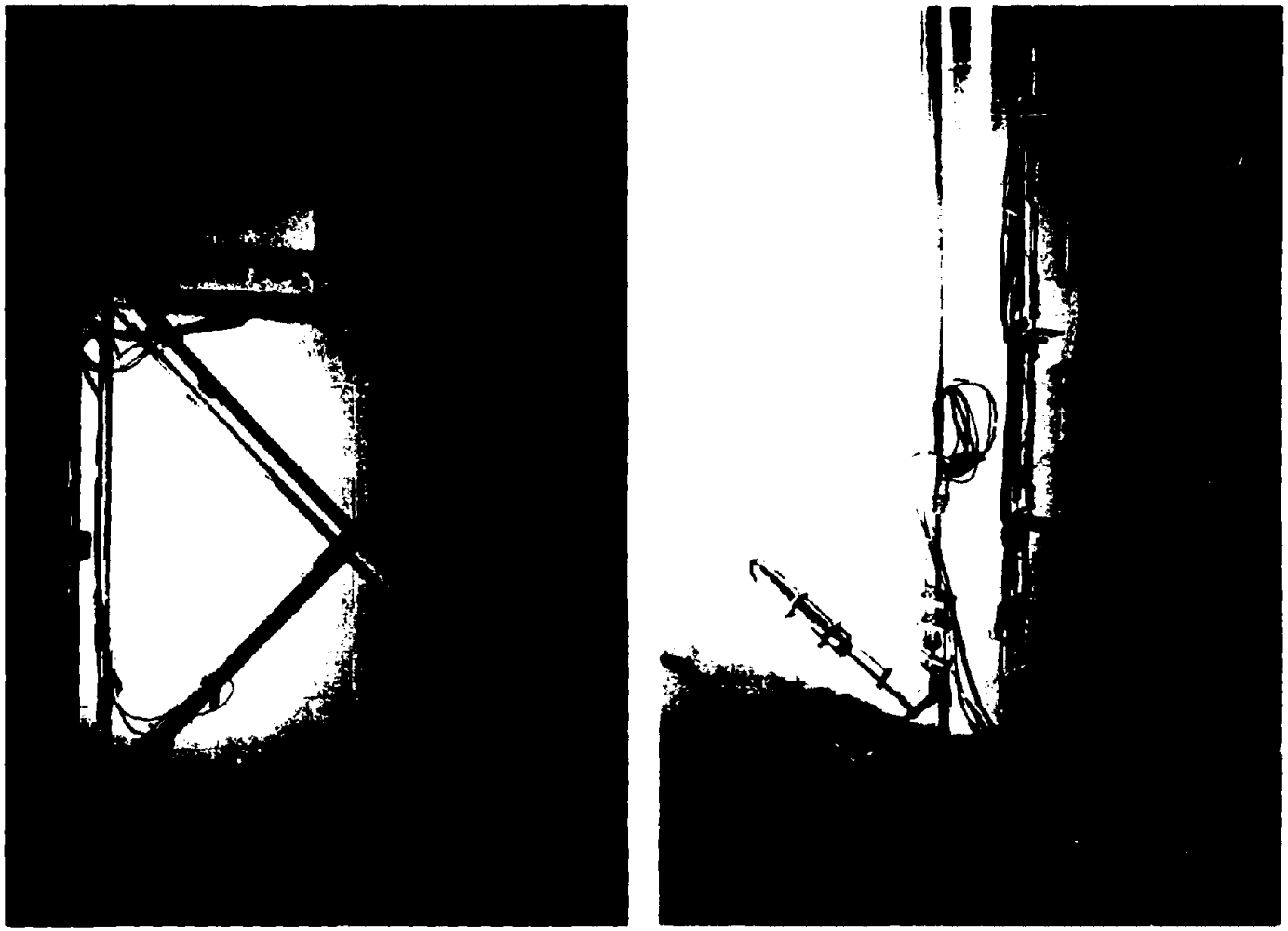

Figure A-7 Typical Wall Panel Deformation and Curvature Instrumentation

Figure A-8 Typical Crack Pattern in Floor Slab Topping at ~0.2% Building Drift

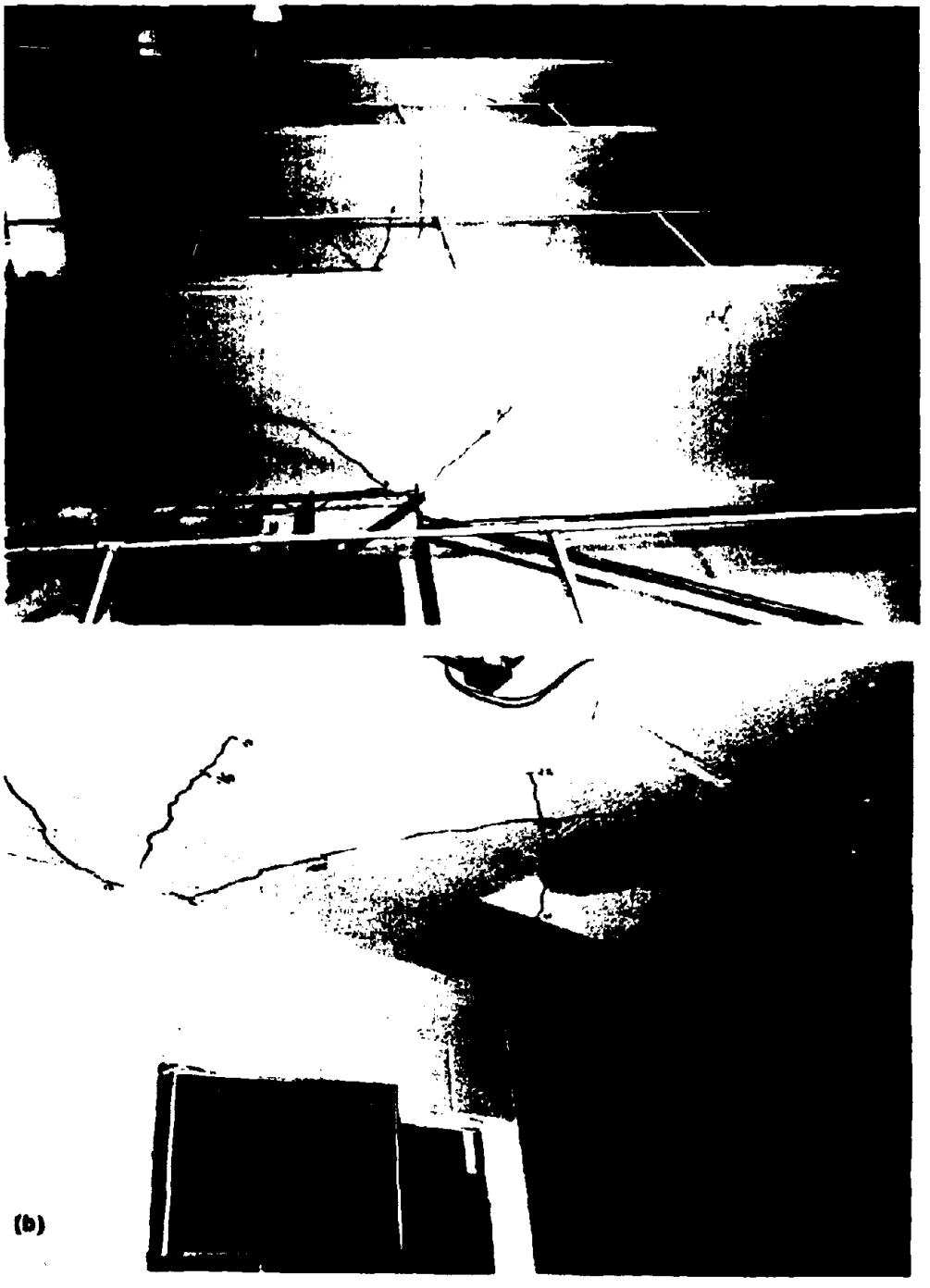

Figure A-9 Typical Crack Pattern in Prestressed Planks at ~0.2% Building Drift

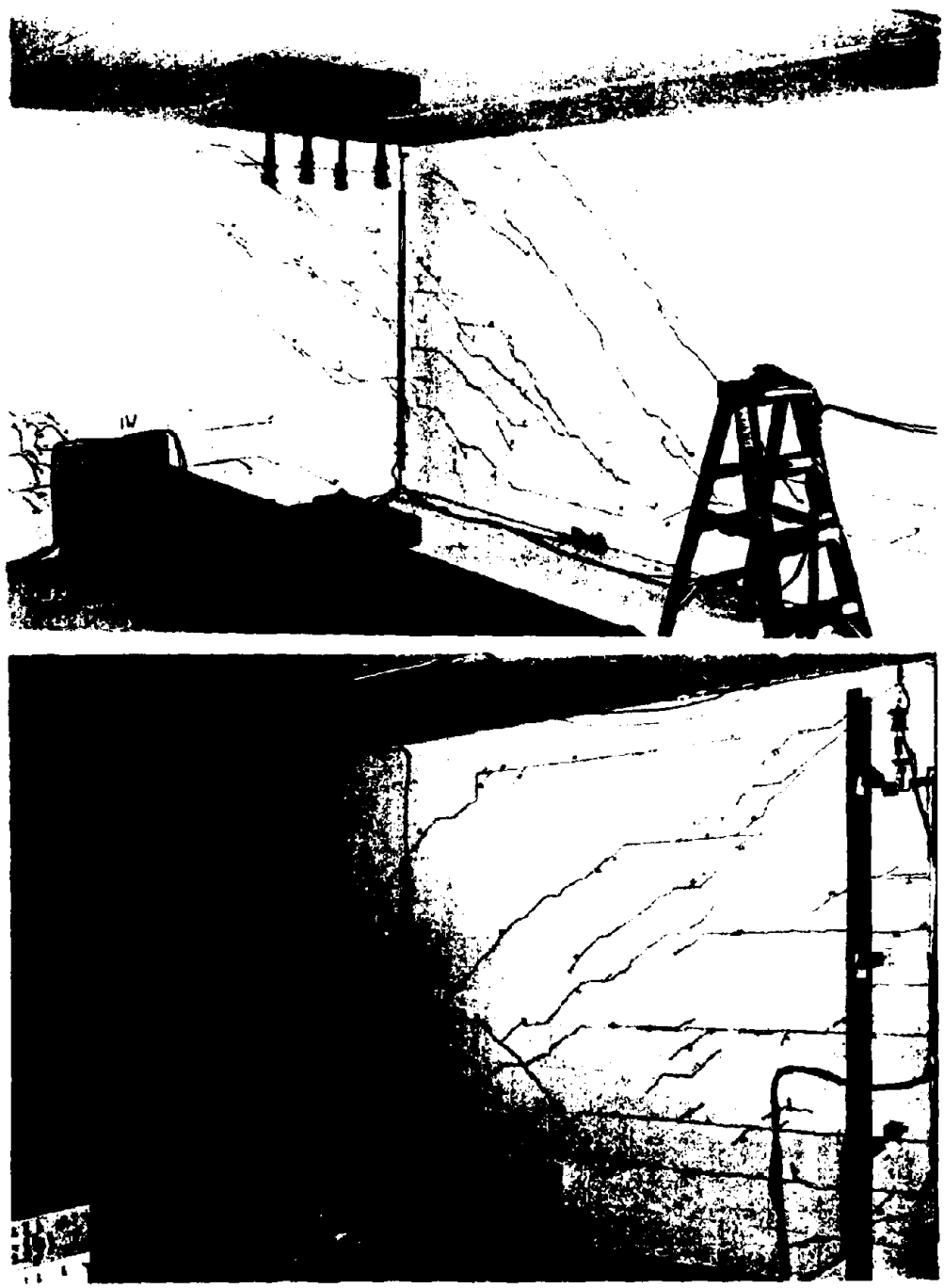

Figure A-10 Crack Pattern in the 1st and 2nd Story Wall and Flange at -0.2% Building Drift

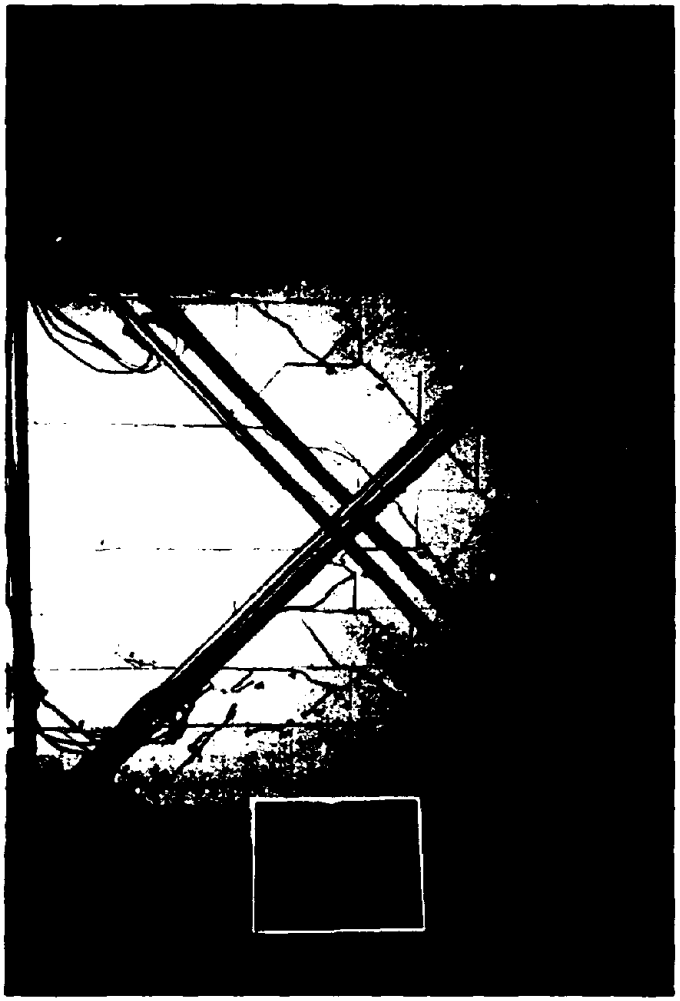

(b) Short T-Wall

(a) Long Flange L-Wall

Figure A-11 1st Story Wall Crack Patterns at ~0.5% Building Drift

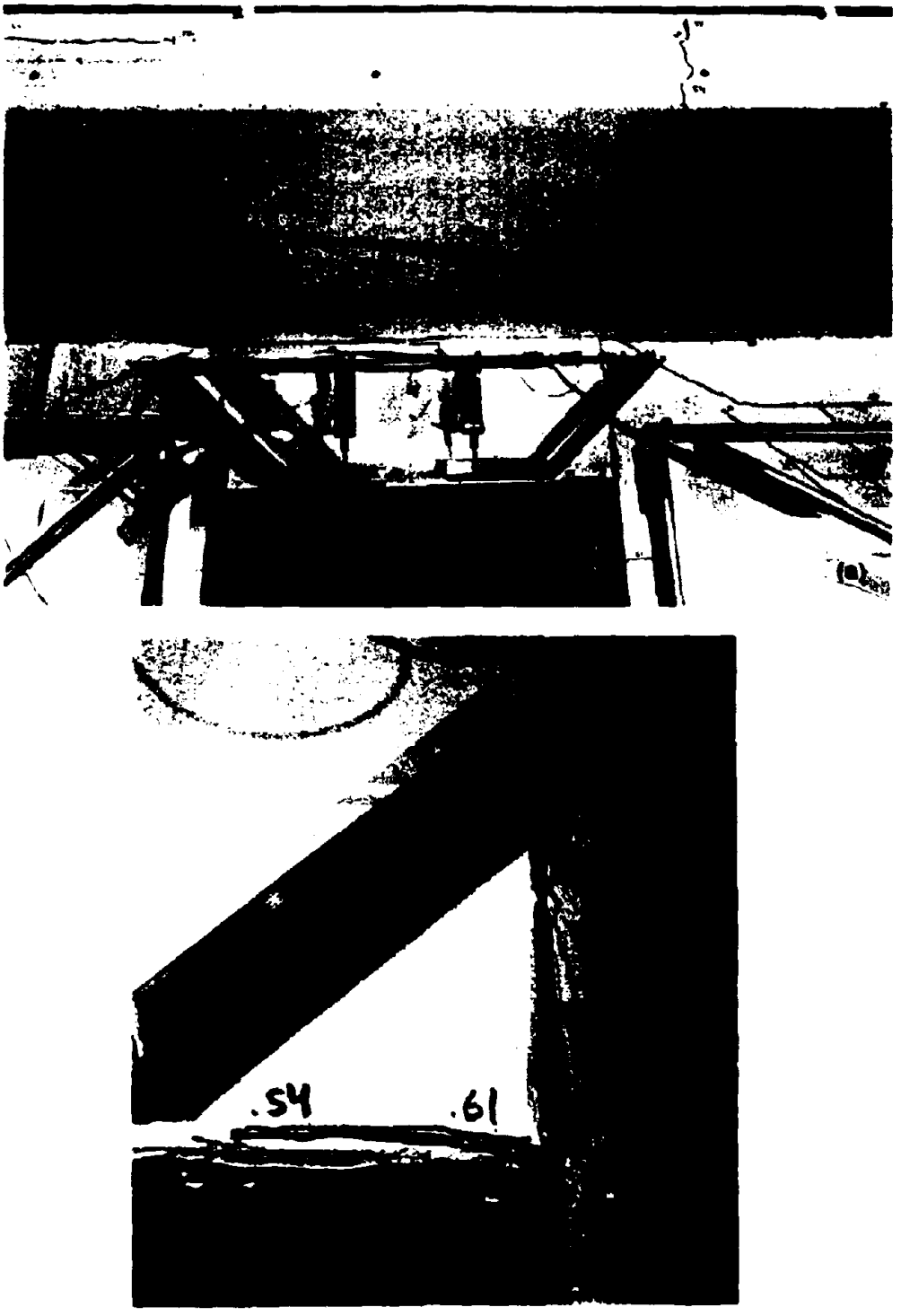

Figure A-12 First Damage at 1st Story Door Lintel at ~0.6% Building Drift

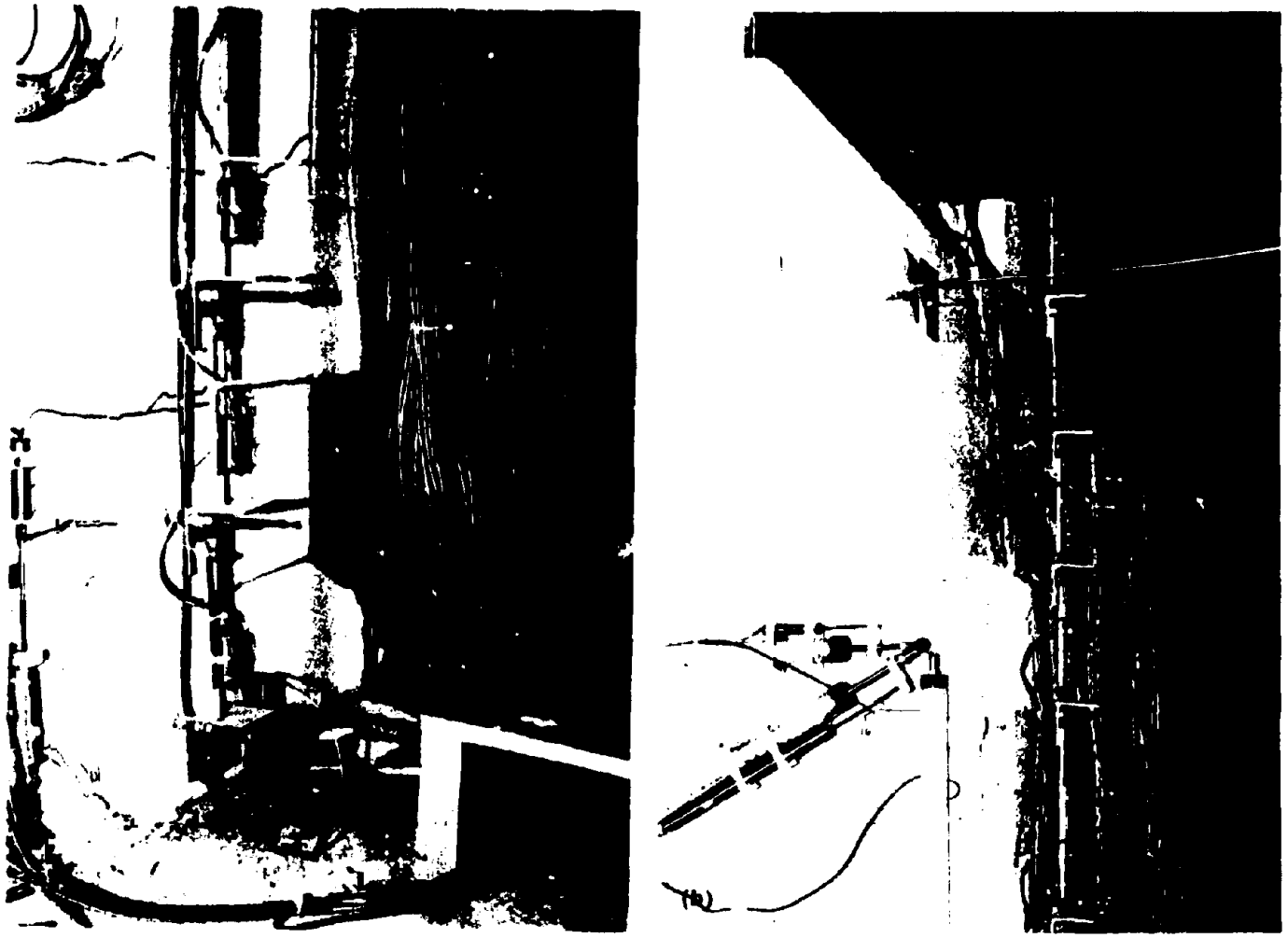

Figure A-13 Vertical Splitting Failure Associated with Wall Sliding at Bottom and Top of 1st Story Long Wall/Flange Intersection

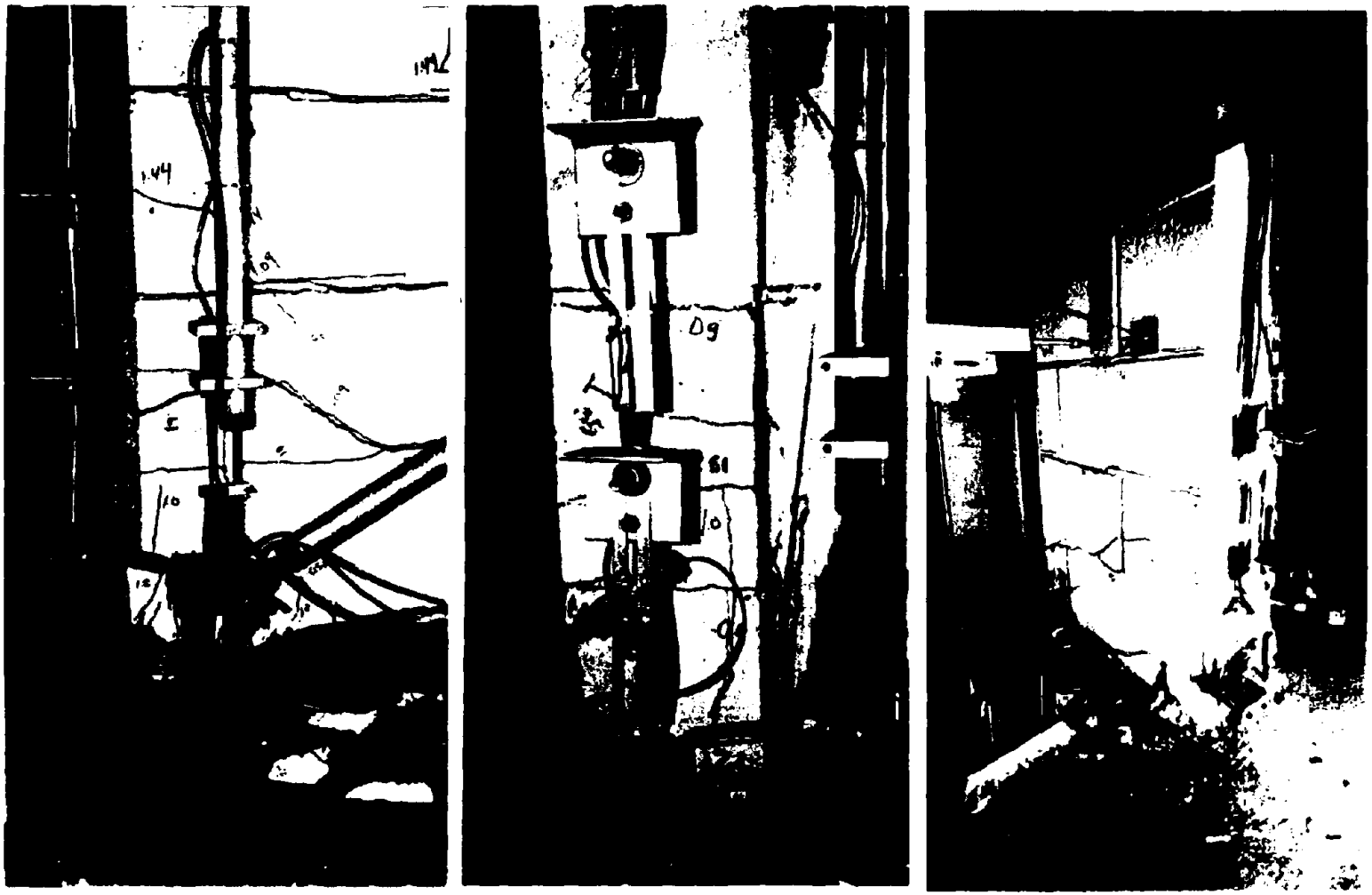

Figure A-14 Ultimate Toe Failure at Long Wall in Push Direction at a Building Drift Angle of 1%

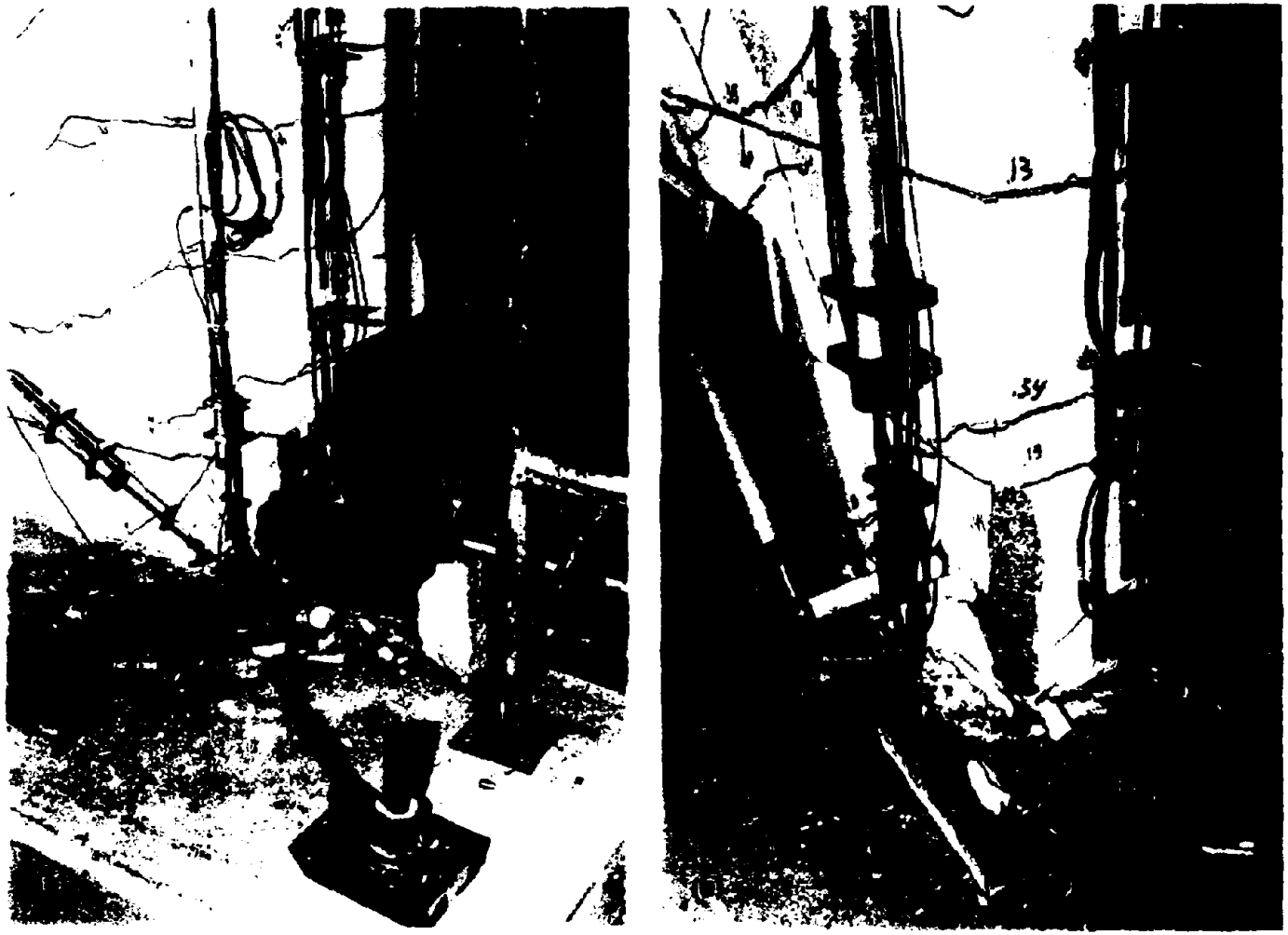

Figure A-15 Ultimate Toe Failure in Pull Direction in 1st Story Long and Short Walls

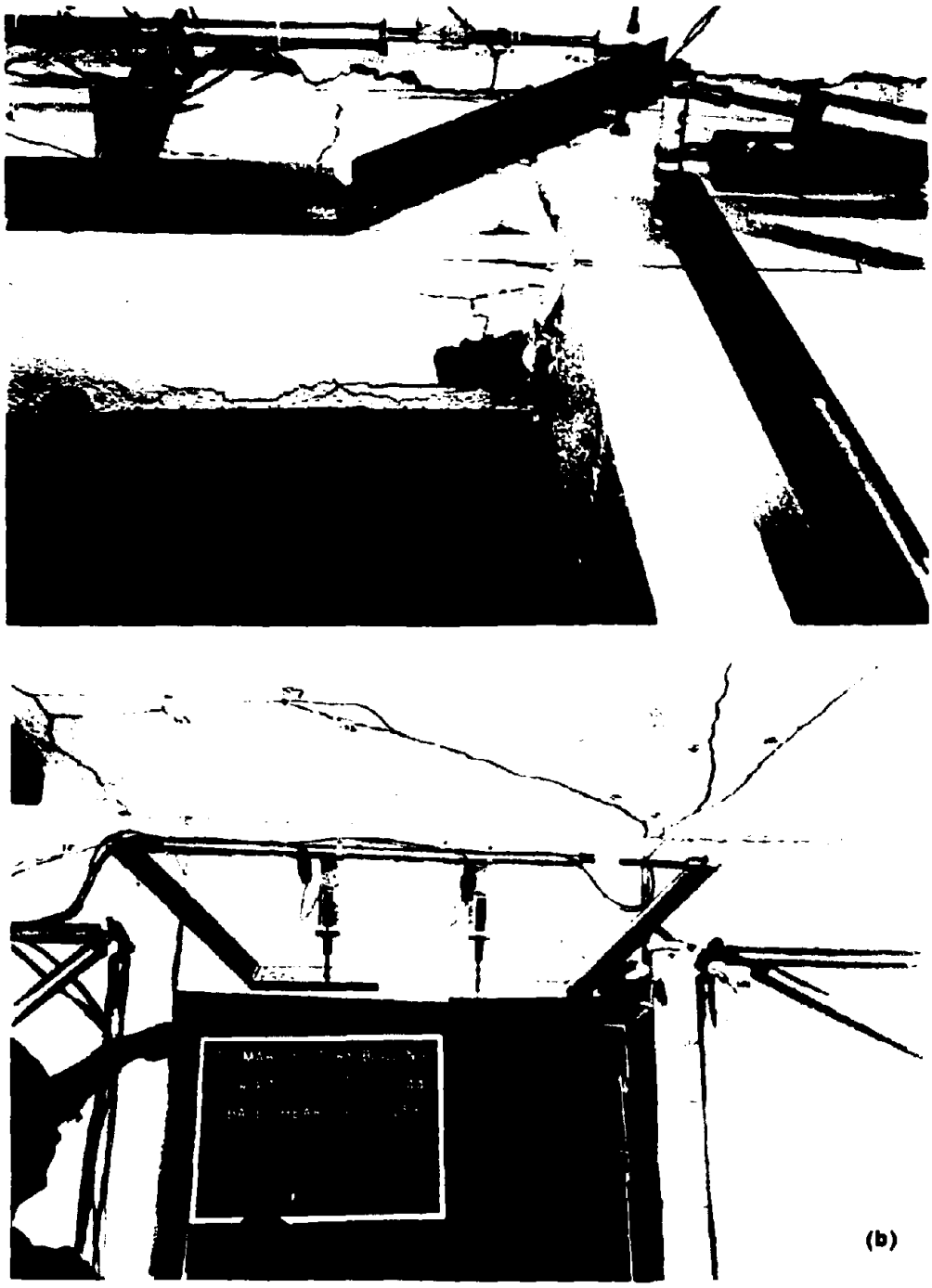

Figure A-16 Ultimate Lintel Damage at Building Drift Angle of 1.44%

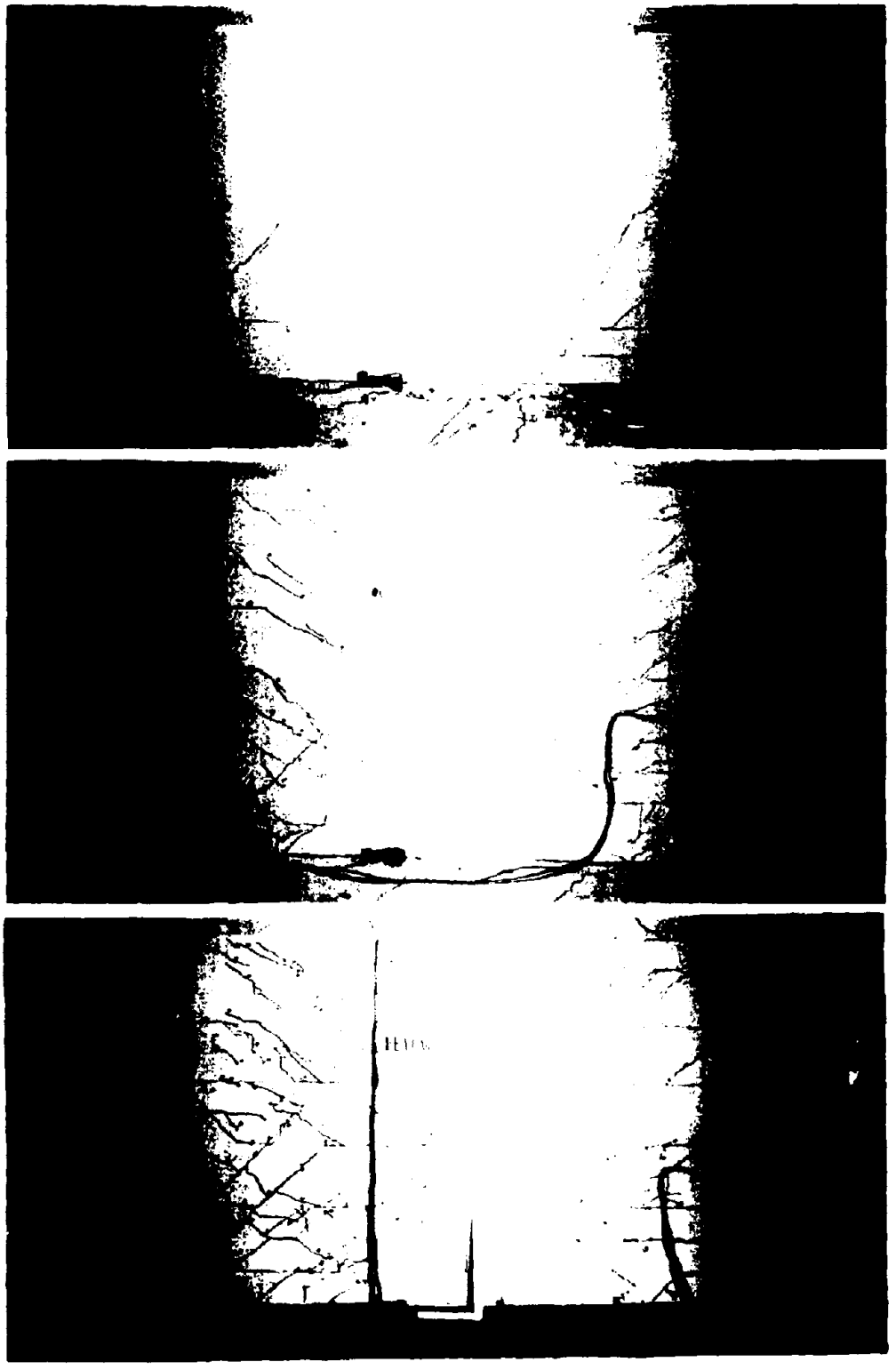

Figure A-17 Ultimate Long Wall Crack Pattern in 1st, 2nd and 3rd Story

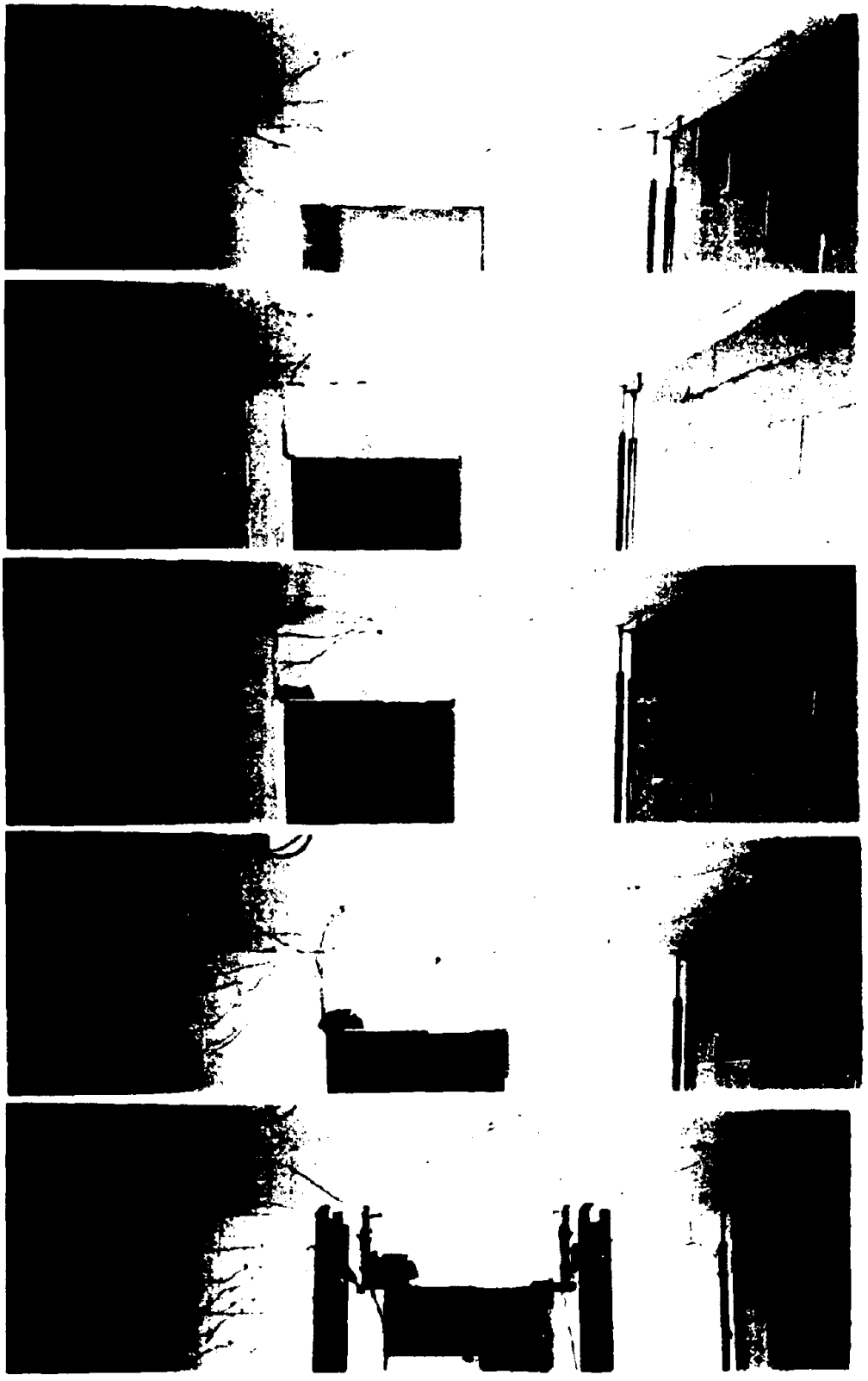

Figure A-18 Ultimate Damage at Doorway and Lintel in all Stories